University of Alberta

THE DEVELOPMENT AND APPLICATIONS OF THE WELL-TEMPERED MODEL CORE POTENTIALS FOR THE MAIN GROUP ELEMENTS

by

Jonathan Y. Mane ©

A thesis submitted to the Faculty of Graduate Studies and Research in partial fulfillment of the requirements for the degree of **Master of Science**

Department of Chemistry

Edmonton, Alberta
Spring 2002

0-612-69735-5

University of Alberta

Library Release Form

Name of Author: Jonathan Y. Mane

Title of Thesis: The Development and Applications of the Well-tempered Model Core Potentials for the Main Group Elements

Degree: Master of Science

Year this Degree Granted: 2002

Jonathan Y. Mane
1575 Dila,
Santa Rosa, Laguna
4026 PHILIPPINES

Date: 07 JAN 2002

University of Alberta

Faculty of Graduate Studies and Research

The undersigned certify that they have read, and recommend to the Faculty of Graduate Studies and Research for acceptance, a thesis entitled **The Development and Applications of the Well-tempered Model Core Potentials for the Main Group Elements** submitted by Jonathan Y. Mane in partial fulfillment of the requirements for the degree of **Master of Science**.

Dr. Mariusz Klobukowski (Supervisor)

Dr. Pierre-Nicholas Roy

Dr. Gerda de Vries

Date: 07 JAN 2002

to my dad Exequiel, my mom Elena and my brother Mong

Abstract

A new family of model core potentials, based on the well-tempered basis set expansion, was developed for the main group elements Li through Rn. For alkali and alkaline-earth metal atoms the valence space includes the ns valence shell and the outermost core (n-1)p shell. For the p-block elements, the valence space comprises the valence ns and np shells together with the (n-1)d shells. The Gaussian exponents are shared between the s- and p-type functions, leading to basis sets with L-shell structure. Non-relativistic MCPs were prepared for all atoms. Scalar-relativistic effects were incorporated in the MCPs for all the atoms heavier than Ar using the relativistic elimination of small components method in order to obtain the core and reference orbitals. The new potentials were tested in molecular calculations at the RHF level and the results were compared with the corresponding values given by the all-electron calculations. Excellent agreement between the wtMCPs and AE results was obtained. Molecular calculations that include electron correlation were also done at the MP2 and DFT levels and results were compared with experimental data. The wtMCP results agree well with experimental data.

Acknowledgements

I would like to thank the persons who made this research project a very successful one. Dr. Mariusz Klobukowski, my research supervisor, for his excellent guidance and support, for providing me the opportunity to be part of his research group as a budding computational chemist and for helping me in solving problems ranging from simple computer to advance theoretical problems. Dr. Pierre-Nicholas Roy and Dr. Gerda de Vries for spending their precious time in reading and evaluating the thesis. Dr. Anna Jordan, my Physical Chemistry Laboratory coordinator, for providing me a flexible time schedule I needed during the writing of the thesis. Christopher Lovallo and John Lo, my research co-workers for their support. Also, my family and friends for their support when I need them.

I would also like to acknowledge the University of Alberta Department of Chemistry for my TA scholarship and for the Linux workstations used in the project, the National Science and Engineering Research Council (NSERC) of Canada for the funding of workstations and; the U of A Computing & Networking Systems (CNS) for the IBM RS6000 servers.

Contents

1 Introduction **1**
- 1.1 Hartree-Fock Method 2
- 1.2 Post Hartree-Fock Methods 6
- 1.3 Density Functional Theory 8
- 1.4 Pseudopotential Methods 10
  - 1.4.1 Model Core Potential 11
  - 1.4.2 Effective Core Potentials 12
  - 1.4.3 Comparison of MCP and ECP models 13
  - 1.4.4 Relativistic Pseudopotentials 13
- 1.5 Basis Sets 14
  - 1.5.1 Slater and Gaussian Type Functions 15
  - 1.5.2 Well-tempered, MCP, and ECP Basis Sets 16

2 The Development of the Well-tempered Model Core Potentials **18**
- 2.1 The Analytical Reference Functions 20
- 2.2 The wtMCP Valence Basis Sets 21
- 2.3 The Optimization Method 22
- 2.4 The Quality of the wtMCP 24

3 The Applications of the wtMCPs in Molecular Calculations **32**
- 3.1 Comparison of All-electron and wtMCP Results 33
  - 3.1.1 Computational Method 33
  - 3.1.2 Results and Discussion 35
- 3.2 Comparison of Experimental and wtMCP Results 44
  - 3.2.1 Computational Method 44
  - 3.2.2 Results and Discussion 46

4 Conclusions and Future Prospects **50**

Bibliography **52**

A Supplementary Tables for Chapter 3 **60**

B Supplementary Figures for Chapter 2 **66**

List of Figures

2.1 Non-relativistic Xe(^{1}S) 5s radial distribution function 25
2.2 Non-relativistic Xe(^{1}S) 5p radial distribution function 26
2.3 Non-relativistic Xe(^{1}S) 4d radial distribution function 27

3.1 Comparison of calculated and experimental bond lengths for diatomic molecules 46
3.2 Comparison of calculated and experimental vibrational frequencies for diatomic molecules 47
3.3 Comparison of calculated and experimental bond lengths for AH_2 and AH_3 molecules 48
3.4 Comparison of calculated and experimental bond angles for AH_2 and AH_3 molecules 49

B.1 Scalar-relativistic Xe(^{1}S) 5s radial distribution function 67
B.2 Scalar-relativistic Xe(^{1}S) 5p radial distribution function 68
B.3 Scalar-relativistic Xe(^{1}S) 4d radial distribution function 69

List of Tables

2.1 Gaussian primitives of AE and wtMCP valence basis sets . . . 23
2.2 Radial expectation values for noble-gas atoms 28
2.3 Static dipole polarizability for the noble-gas atoms 31

3.1 Contraction patterns of the AE and wtMCP basis sets 34
3.2 Optimized geometries of homonuclear diatomic molecules . . . 35
3.3 Vibrational frequencies for diatomic molecules 36
3.4 Results for A_3^- ions 37
3.5 Results for AF_3 molecules 38
3.6 Results for AF_5 molecules 40
3.7 Results for AF_7 molecules 41
3.8 Results for noble-gas fluorides 43
3.9 wtMCP basis set contractions used in correlation studies . . . 45

A.1 Bond lengths and vibrational frequencies for group 13 halides . 61
A.2 Bond lengths and vibrational frequencies for group 14 sulfides 62
A.3 Bond lengths and vibrational frequencies for diatomic interhalogen compounds 63
A.4 Bond lengths and bond angles for dihydrogen chalcogenides . . 64
A.5 Bond lengths and bond angles for trihydrogen pnictides 65

List of Abbreviations

AE	all-electron
AO	atomic orbital
ax	axial
cGTF	contracted Gaussian-type function
DFT	density functional theory
ECP	effective core potential
eq	equatorial
GTF	Gaussian-type function
HF	Hartree-Fock
KS	Kohn-Sham
MCP	model core potential
MP2	second-order Møller-Plesset perturbation
MP3	third-order Møller-Plesset perturbation
NR-wtMCP	non-relativistic model core potential
pGTF	primitive Gaussian-type function
RESC	relativistic elimination of small components
RHF	restricted Hartree-Fock
ROHF	restricted open-shell Hartree-Fock
SCF	self consistent field
SR-wtMCP	scalar-relativistic well-tempered model core potential
STF	Slater-type function
WTBS	well-tempered basis set
wtMCP	well-tempered model core potential
XC	exchange-correlation

Chapter 1

Introduction

Computational chemistry has become one of the most popular tools in modern chemistry. It uses theoretical models that have been developed over the past three decades and exploits the number-crunching capabilities of modern computers. With an increasing trend in performance-to-cost ratio of computers, simulating experiments using computers has advantages - reduction in operating expenses and increased safety in doing experiments by avoiding expensive and toxic chemicals. By using computers, it is possible to simulate experiments which may be very difficult or even impossible to do in even the most sophisticated laboratory.

Today, computational chemistry has become a widely used tool and an integral part of scientific investigation. It often works side by side with experimental chemistry to develop better theoretical models with more accurate predicting power. It is used in explaining some puzzling experimental results. In order to achieve such high accuracy, the development of new methods and/or improving the capabilities of existing ones is necessary.

The quality of results from modern *ab initio* calculations relies heavily both on the method used as well as on the quality of basis set used. There are numerous existing basis sets that have been developed as can be seen later in this chapter. In this thesis, a development of a new family of basis sets has been done, and described in later chapters.

In this chapter, an introduction to the theories and methods relevant to the development of the new basis set is discussed. First, a simple description of Hartree-Fock theory and post Hartee-Fock methods is presented. It is then followed by a brief discussion on pseudopotential theory. Finally, a discussion of basis sets is presented. The detailed description and derivation of formulas presented here can be found in many standard quantum chemical textbooks. The major references used here include the books by Szabo and Ostlund[1], Levine[2], Jensen[3] and McQuarrie[4].

1.1 Hartree-Fock Method

One of the major challenges for quantum chemists is finding an exact solution to the non-relativistic time-independent Schrödinger equation

$$\hat{H}\Psi(R_A, r_i) = E\Psi(R_A, r_i) \quad (1.1)$$

which yields, upon solving, the wavefunctions Ψ and energies E. In Eq. (1.1), $\hat{H}$ is the Hamiltonian operator for a system of nuclei and electrons described by the position vectors R_A and r_i, respectively, and is given in atomic units as

$$\hat{H} = -\sum_{A=1}^{M}\frac{1}{2M_A}\nabla_A^2 - \sum_{i=1}^{N}\frac{1}{2}\nabla_i^2 - \sum_{i=1}^{N}\sum_{A=1}^{M}\frac{Z_A}{r_{iA}} + \sum_{i=1}^{N}\sum_{j>i}^{N}\frac{1}{r_{ij}} + \sum_{A=1}^{M}\sum_{B>A}^{M}\frac{Z_A Z_B}{R_{AB}}. \quad (1.2)$$

The first term in Eq. (1.2) is the operator for the kinetic energy of the nuclei, $\hat{T}_N$. The second term is the operator for the kinetic energy of the electrons, $\hat{T}_e$. The third term represents the Coulomb attraction between the electrons and the nuclei, $\hat{V}_{Ne}$, where r_{iA} is the distance between electron i and nucleus A. The fourth and fifth terms are $\hat{V}_{ee}$, the potential energy of repulsions between electrons i and j separated by a distance r_{ij}, and $\hat{V}_{NN}$, the potential energy of repulsions between nuclei A and B separated by a distance R_{AB}, respectively.

Eq. (1.1) is very difficult to solve and approximations must be made. The key to simplifying the solution to Eq. (1.1) is to separate the electronic from the nuclear degrees of freedom. This approximation, known as the *Born-Oppenheimer approximation*, says that the true molecular wavefunction can be approximated as:

$$\Psi(R_A, r_i) = \Psi_{el}(r_i; R_A)\Psi_N(R_A). \quad (1.3)$$

The electrons are much lighter and so they move much faster than the nuclei. During the entire electronic motion, the nuclei move very slowly and the effects of nuclear motion can be considered negligible. Hence, we can think of the electrons in a molecule as moving in the field of fixed nuclei. Within the Born-Oppenheimer approximation, $\hat{T}_N$ can be neglected and $\hat{V}_{NN}$ can be considered constant since the nuclear positions are fixed. Since $\hat{V}_{NN}$ is a constant, it does not affect the electronic wavefunction; it only adds up to the energy eigenvalue. Therefore, we can write the electronic Schrödinger equation as

$$(\hat{H}_{el} + \hat{V}_{NN})\Psi_{el} = E_{tot}\Psi_{el} \quad (1.4)$$

where

$$\hat{H}_{el} = -\sum_{i=1}^{N}\frac{1}{2}\nabla_i^2 - \sum_{i=1}^{N}\sum_{A=1}^{M}\frac{Z_A}{r_{iA}} + \sum_{i=1}^{N}\sum_{j>i}^{N}\frac{1}{r_{ij}} \quad (1.5)$$

$$\hat{V}_{NN} = \sum_{A=1}^{M}\sum_{B>A}^{M}\frac{Z_A Z_B}{R_{AB}} \quad (1.6)$$

$$E_{tot} = E_{el} + V_{NN}. \quad (1.7)$$

Omitting $\hat{V}_{NN}$ from Eq. (1.4), a purely electronic Schrödinger equation is obtained, *i.e.*

$$\hat{H}_{el}\Psi_{el} = E_{el}\Psi_{el} \tag{1.8}$$

Ψ_{el} is the electronic wavefunction describing the motion of N electrons in the field of M point charges. Both Ψ_{el} and E_{el} depend *parametrically* on the nuclear configuration:

$$\Psi_{el} = \Psi_{el}(\{R_A\}) \tag{1.9}$$
$$E_{el} = E_{el}(\{R_A\}). \tag{1.10}$$

This means that for different arrangements of the nuclei, there are different values for Ψ_{el} and E_{el}. Equations (1.9) and (1.10) make it possible to define the potential energy surface of a molecule as a function of nuclear coordinates.

Although Eq. (1.5) is simplified, it still contains a many-body Hamiltonian and is very difficult to solve. Analytic solutions exist only for systems having one electron. The *Hartree-Fock(HF) method* offers a very popular approach to solving the many-body eigenvalue problem. The method allows to transform the full N-body equation into N single-body equations.

For a closed-shell system involving *fermions* such as electrons, the ground-state Hartree-Fock wavefunction is given by a single antisymmeterized function, the Slater determinant, of N spin-orbitals, $\psi_i(\mathbf{x}_j)$:

$$\Psi_0 = \frac{1}{\sqrt{N!}}\begin{vmatrix} \psi_1(\mathbf{x}_1) & \psi_1(\mathbf{x}_2) & \dots & \psi_1(\mathbf{x}_N) \\ \psi_2(\mathbf{x}_1) & \psi_2(\mathbf{x}_2) & \dots & \psi_2(\mathbf{x}_N) \\ \vdots & \vdots & \ddots & \vdots \\ \psi_N(\mathbf{x}_1) & \psi_N(\mathbf{x}_2) & \dots & \psi_N(\mathbf{x}_N) \end{vmatrix} = |\psi_1(\mathbf{x}_1)\psi_2(\mathbf{x}_2)\cdots\psi_N(\mathbf{x}_N)\rangle \tag{1.11}$$

where the variable $\mathbf{x}$ corresponds to space, $\mathbf{r}$, and spin coordinates, σ. The spin-orbital, $\psi_i(\mathbf{x}_j)$, is a simple product of space and spin functions, α and β:

$$\psi_i(\mathbf{x}_j) = \phi_i(\mathbf{r}_j) \times \left\{ \begin{array}{c} \alpha(\sigma_j) \\ \beta(\sigma_j) \end{array} \right. . \tag{1.12}$$

According to the variational principle, the best wavefunction Ψ_0 is the one that minimizes the ground state energy, E_0:

$$E_0 = \left\langle \Psi_0 \left| \hat{H}_{el} \right| \Psi_0 \right\rangle . \tag{1.13}$$

Using the wavefunction in Eq. (1.11) in Eq. (1.13), the energy E_0 becomes a functional of the spin-orbitals, $\psi_i(\mathbf{x}_j)$. Finding the best spin-orbitals which minimize E_0 corresponds to finding the best possible approximation to the ground state of the N-electron system described by $\hat{H}_{el}$. Such an approximation, which reduces the problem of N-electron equations to a set of 1-electron eigenvalue equations, is known as the Hartree-Fock equation:

$$\hat{F}(\mathbf{x}_1)\psi_i(\mathbf{x}_1) = \epsilon_i\psi_i(\mathbf{x}_1), \qquad i = 1, 2, \dots, N. \tag{1.14}$$

Furthermore, by exploiting the orthonormality of the spin-orbitals, the HF equation can be written in terms of spatial orbitals:

$$\hat{F}(1)\phi_i(1) = \epsilon_i\phi_i(1), \qquad i = 1, 2, \ldots, N \tag{1.15}$$

where 1 represents the spatial coordinates of the electron under consideration, here taken to be labeled by 1. In Eq. (1.15), $\hat{F}(1)$ is the effective one-electron operator called the *Fock* (or *Hartree-Fock*) *operator*, $\phi_i(1)$ is the ith spatial orbital and the eigenvalue ϵ_i is the *orbital energy* of spatial orbital ϕ_i. The Fock operator can be expressed as

$$\hat{F}(1) = \hat{h}^{core}(1) + \hat{v}^{HF}(1). \tag{1.16}$$

The term $\hat{h}^{core}(1)$, the *core-Hamiltonian operator*, describes the motion of a single electron in the field of all other nuclei. It consists of the operator for the kinetic energy of one electron, and potential-energy operators for the attraction between one electron and the nuclei:

$$\hat{h}^{core}(1) = -\frac{1}{2}\nabla_1^2 - \sum_{A=1}^{M}\frac{Z_A}{r_{1A}}. \tag{1.17}$$

The term $\hat{v}^{HF}(1)$, the *Hartree-Fock potential operator*, models electron-electron interaction. For a closed-shell system, it is defined as:

$$\hat{v}^{HF}(1) = \sum_{j=1}^{N/2}\left[2\hat{J}_j(1) - \hat{K}_j(1)\right] \tag{1.18}$$

where $\hat{J}_j(1)$ and $\hat{K}_j(1)$ are the Coulomb and exchange operators, respectively. The sum over j runs over the occupied spatial orbitals ϕ_i of the N-electron molecule. The Coulomb and exchange operators are defined as:

$$\hat{J}_j(1)\phi_i(1) = \left[\int \frac{|\phi_j(2)|^2}{r_{12}} d\mathbf{r}_2\right]\phi_i(1) \tag{1.19}$$

$$\hat{K}_j(1)\phi_i(1) = \left[\int \frac{\phi_j^*(2)\phi_i(2)}{r_{12}} d\mathbf{r}_2\right]\phi_j(1). \tag{1.20}$$

The Coulomb operator $\hat{J}_j(1)$ represents the average repulsion experienced by electron 1 due to the charge distribution associated with electron 2. The exchange operator $\hat{K}_j(1)$ represents of the electrostatic interaction of two overlapping charge densities. It arises from the antisymmetry requirement imposed on the total wavefunction Ψ with respect to electron interchange and has no classical interpretation.

The HF equation is a differential equation in which the Fock operator, $\hat{F}$, depends on its own eigenfunction. Solving the HF equation requires the knowledge of the wavefunction. However, the wavefunction is not known initially. In cases such as this, the problem must be solved iteratively. This is usually done by using an initial guess to the wavefunction to calculate the new wavefunction. Then, one takes the new wavefunction as the next guess. The procedure is repeated until the old and the new wavefunctions do not differ. This method is known as the *self-consistent field (SCF) method.* The problem of solving the HF differential equation was made possible by expanding the spatial orbitals ϕ_i as a linear combination of a known set of K one-electron basis function χ_β [5]:

$$\phi_i(1) = \sum_{\beta=1}^{K} \chi_\beta(1) c_{\beta i}. \tag{1.21}$$

Substituting Eq. (1.21) into the HF equation (1.15) gives

$$\hat{F}_i(1) \sum_{\beta=1}^{K} \chi_\beta(1) c_{\beta i} = \epsilon_i \sum_{\beta=1}^{K} \chi_\beta(1) c_{\beta i} \tag{1.22}$$

which, after multiplying from the left by a specific basis function, *e.g.*, χ_α, and integration, gives the Hartree-Fock-Roothaan-Hall (HFRH) equations[6]

$$\sum_{\beta=1}^{K} (F_{\alpha\beta} - \epsilon S_{\alpha\beta}) c_{\beta i} = 0 \qquad \alpha = 1, 2, \ldots, K. \tag{1.23}$$

Eq. (1.23) can be conveniently represented in matrix notation as:

$$\mathbf{FC} = \mathbf{SC}\epsilon. \tag{1.24}$$

The $\mathbf{F}$ matrix contains the elements $F_{\alpha\beta}$

$$F_{\alpha\beta} \equiv \left\langle \chi_\alpha(1) \left| \hat{F}(1) \right| \chi_\beta(1) \right\rangle \tag{1.25}$$

$$= \left\langle \chi_\alpha \left| \hat{h}^{core} \right| \chi_\beta \right\rangle + \sum_{i=1}^{N/2} \left[2 \left\langle \chi_\alpha \left| \hat{J}_i \, \chi_\beta \right. \right\rangle - \left\langle \chi_\alpha \left| \hat{K}_i \, \chi_\beta \right. \right\rangle \right]. \tag{1.26}$$

The $\mathbf{S}$ matrix contains the overlap of elements $S_{\alpha\beta}$ between basis function

$$S_{\alpha\beta} \equiv \langle \chi_\alpha(1) \mid \chi_\beta(1) \rangle ; \tag{1.27}$$

$\mathbf{C}$ is a $K \times K$ square matrix of the expansion coefficients $c_{\beta i}$

$$\mathbf{C} = \begin{pmatrix} c_{11} & c_{12} & \cdots & c_{1K} \\ c_{21} & c_{22} & \cdots & c_{2K} \\ \vdots & \vdots & \ddots & \vdots \\ c_{K1} & c_{K2} & \cdots & c_{KK} \end{pmatrix}, \tag{1.28}$$

and ϵ is a diagonal matrix of the orbital energies ϵ_i

$$\epsilon = \begin{pmatrix} \epsilon_1 & 0 & \cdots & 0 \\ 0 & \epsilon_2 & \cdots & 0 \\ \vdots & \vdots & \ddots & \vdots \\ 0 & 0 & \cdots & \epsilon_K \end{pmatrix}. \tag{1.29}$$

The solution to Eq. (1.24) requires finding the matrix $\mathbf{C}$ and ϵ. In solving the HFRH equation via the SCF procedure, an initial guess of the expansion coefficients $c_{\beta i}$ is made to form the Fock matrix. The Fock matrix is then diagonalized to obtain a new set of coefficients which is then used for forming the new Fock matrix. The procedure is repeated until there are no more changes between the old and the new set of coefficients within some given threshold. The converged set of coefficients constitutes the SCF solution.

The generalized HF energy (or the total energy) of any closed shell system using N-occupied orbitals is:

$$E_{HF} = 2\sum_{i=1}^{N/2} \hat{h}_{ii}^{core} + \sum_{i=1}^{N/2}\sum_{j=1}^{N/2}(2\langle ij \mid ij\rangle - \langle ij \mid ji\rangle) + \sum_{A=1}^{M}\sum_{B>A}^{M} \frac{Z_A Z_B}{R_{AB}} \tag{1.30}$$

where

$$\hat{h}_{ii}^{core} \equiv \left\langle \phi_i(1) \left| \hat{h}^{core}(1) \right| \phi_i(1) \right\rangle \tag{1.31}$$

$$\langle ij \mid ij\rangle \equiv \left\langle \phi_i(1)\phi_j(2) \left| \frac{1}{r_{12}} \right| \phi_i(1)\phi_j(2) \right\rangle = J_{ij} \tag{1.32}$$

$$\langle ij \mid ji\rangle \equiv \left\langle \phi_i(1)\phi_j(2) \left| \frac{1}{r_{12}} \right| \phi_j(1)\phi_i(2) \right\rangle = K_{ij}. \tag{1.33}$$

In a closed shell system, restricting each spatial orbitals to have two electrons, one with α and one with β spin, is known as the *Restricted Hartree-Fock* (RHF) method. For open shell systems, it is known as the *Restricted Open-shell Hartree-Fock* (ROHF) method.

1.2 Post Hartree-Fock Methods

The Hartree-Fock wavefunction is a good approximation to the many-body wavefunction for solving the Schrödinger equation. Although the HF method treats electron interaction in an average way, it is able to account for about 99% of the total energy of the system using a sufficiently large basis. In order to improve the HF approximation, instantaneous electron-electron interaction, *i.e. electron correlation*, must also be considered. The effect of the electrons being correlated is often described by the electron correlation energy, E_{corr}. E_{corr} is defined as the difference between the exact nonrelativistic energy of the system, (E_{NR}) and the HF energy, (E_{HF}), obtained by using a sufficiently large basis set,

$$E_{corr} \equiv E_{NR} - E_{HF} \tag{1.34}$$

A general method of improving the HF results is to consider more than one Slater determinant, Eq. (1.11), for the exact wavefunction. Such determinants may be constructed using the solutions of the HFRH equations. By solving the Roothaan-Hall equation of a closed-shell N-electron system using K basis functions, there are $2K$ spin-orbitals of which N are occupied and $(2K - N)$

are virtual spin-orbitals. From these $2K$ spin-orbitals, a large number of determinants can be formed. Among these determinants, aside from the N lowest energy spin orbitals, $|\Phi_{HF}\rangle \equiv |\Phi_0\rangle$, are singly, $|\Phi_i^a\rangle$, doubly, $|\Phi_{ij}^{ab}\rangle$, etc., up to n-tuply excited determinants. These determinants can be used as a basis to expand the exact wavefunction:

$$|\Psi\rangle = c_0|\Phi_0\rangle + \sum_{ia} c_i^a|\Phi_i^a\rangle + \sum_{i<j;\ a<b} c_{ij}^{ab}|\Phi_{ij}^{ab}\rangle + \cdots \tag{1.35}$$

The determinants $|\Phi_0\rangle$, $|\Phi_i^a\rangle$, ..., are kept fixed, while the coefficients c_i are optimized. The best possible expansion coefficients c's are determined and the way they are calculated varies from one method to another. If the coefficient c_0 is large *i.e.*, close to 1, the HF wavefunction is a good representation of the true wavefunction.

There are several techniques for calculating electron correlation that have been reviewed[7, 8, 9]. Very commonly used among these methods are *configuration interaction* (CI), *coupled-cluster* (CC) and *perturbation theory* (PT). Only the perturbation theory is discussed here since the other methods are not used in this thesis. For a discussion of CI, see Ref. [1] and for a review of the CC method, see Ref. [10].

Estimating the electron correlation energy based on perturbation theory was one of the earliest post-HF procedures. The basic idea is that if there are two Hamiltonian operators that are fairly close to each other, for one of which the exact solution is known, then the difference between them is a small perturbation to the solvable Hamiltonian operator.

The *Møller-Plesset perturbation theory* (MPPT)[11] is commonly used in approximating the electron correlation energy. Recalling from Eq. (1.5), the true nonrelativistic electronic Hamiltonian ($\hat{H}_{el} \equiv \hat{H}$) for an N-electron system can be rewritten as:

$$\hat{H} = \sum_{i=1}^{N} \hat{h}^{core}(i) + \sum_{i=1}^{N}\sum_{j>i}^{N} \frac{1}{r_{ij}} \tag{1.36}$$

which takes into account all electron correlation. If the HF wavefunction corresponds to the unperturbed Hamiltonian, $\hat{H}^{(0)}$,

$$\hat{H}^{(0)} = \sum_{i=1}^{N} \hat{F}(i) = \sum_{i=1}^{N} \left[\hat{h}^{core}(i) + v^{HF}(i)\right] \tag{1.37}$$

then electron correlation is seen merely as a perturbation

$$\hat{H}' = \hat{H} - \hat{H}^{(0)} = \sum_{i=1}^{N}\sum_{j>i}^{N} \frac{1}{r_{ij}} - \sum_{j=1}^{N}\sum_{m=1}^{N} \left[\hat{J}_m(j) - \hat{K}_m(j)\right]. \tag{1.38}$$

The second-order Møller-Plesset perturbation theory (MP2) is widely used in molecular calculations because it is relatively inexpensive and usually gives a reasonable portion of the correlation energy. For the ground state of a molecule, this energy is given as

$$E_0^{(2)} = \sum_{i<j}^{occ} \sum_{a<b}^{vir} \frac{[\langle ij \mid ab\rangle - \langle ij \mid ba\rangle]^2}{\epsilon_i + \epsilon_j - \epsilon_a - \epsilon_b} \tag{1.39}$$

where the shorthand notation similar to Eqs. (1.32) and (1.33) for the two electron integrals has been used. For third- and fourth-order MP energy correction formulas, see derivation by Krishnan and Pople[12].

1.3 Density Functional Theory

Post-Hartree-Fock methods are very good in approximating the exact solution to the Schrödinger equation. However, even for small molecular systems calculations are very expensive and time consuming especially if a very large basis set is used. This problem has been addressed by another popular and powerful method called the *density functional theory*(DFT). In the DFT, the system is described by the electron density ρ which depends only on three variables x, y and z. No matter how large the system is, the problem is always 3-dimensional and not $3N$-dimensional as in the HF-based methods. The description of a system from a wave functional approach to density functional approach offers a tremendous reduction in computational effort needed to understand electronic properties of molecular systems.

Hohenberg and Kohn[13] proved in 1964 that for N interacting electrons moving in an external potential $v(\mathbf{r}_i)$, there is a universal functional $F[\rho(\mathbf{r})]$ of the ground-state electron density $\rho(\mathbf{r})$ that minimizes the energy functional

$$E[\rho(\mathbf{r})] = F[\rho(\mathbf{r})] + \int \rho(\mathbf{r})v(\mathbf{r}_i)d\mathbf{r} \tag{1.40}$$

The minimum value of the functional E is E_0, the ground-state electronic energy. The theory is exact only for a nondegenerate ground-state. For a discussion on degenerate ground-states, see Parr and Yang[14].

The major problem with the above theory is that neither the functional $F[\rho(\mathbf{r})]$ is known nor the ways of finding $\rho(\mathbf{r})$ without first finding the wavefunction. In 1965, Kohn and Sham[15] extended the applicability of the Hohenberg and Kohn theorem by devising a practical method for finding $\rho(\mathbf{r})$. This is known as the *Kohn-Sham* (KS) equation, which is very similar to the Hartree-Fock equation:

$$\hat{F}^{KS}\phi_i^{KS}(\mathbf{r}) = \epsilon_i^{KS}\phi_i^{KS}(\mathbf{r}) \tag{1.41}$$

where $\hat{F}^{KS}$ is the effective one-electron Kohn-Sham operator, $\phi_i^{KS}(\mathbf{r})$ are Kohn-Sham orbitals and ϵ_i are Kohn-Sham orbital energies. The interpretation of Kohn-Sham orbitals and orbital energies was discussed by Stowasser and Hoffmann[16]. A comparison of HF and KS determinants as wave functions was discussed by Bouř[17]. The Kohn-Sham orbitals, just like in the Hartree-Fock model, can be expanded as a linear combination of a set of K basis functions, χ_α

$$\phi_i^{KS}(\mathbf{r}) = \sum_{\alpha=1}^{K} \chi_\alpha(\mathbf{r}) c_{\alpha i} \tag{1.42}$$

where the expansion coefficients $\{c_{\alpha i}\}$ are found iteratively.

In the Kohn-Sham formalism, the electron density of the system is calculated as:

$$\rho(\mathbf{r}) = 2\sum_{i=1}^{N/2} |\phi_i(\mathbf{r})|^2 . \tag{1.43}$$

The Kohn-Sham operator, $\hat{F}^{KS}(1)$, is defined as

$$\hat{F}^{KS}(1) = -\frac{1}{2}\nabla_1^2 - \sum_{A=1}^{M} \frac{Z_A}{r_{1A}} + 2\sum_{j=1}^{N/2} J_j + V_{XC}(\mathbf{r}) \tag{1.44}$$

where J_j is the Coulomb repulsion term

$$J_j(\mathbf{r}_1) = \int \frac{\rho(\mathbf{r}_2)}{r_{12}} dv_2 \tag{1.45}$$

and $V_{XC}(\mathbf{r})$ is the exchange-correlation potential term

$$V_{XC}(\mathbf{r}) = \frac{\delta E_{XC}[\rho(\mathbf{r})]}{\delta \rho(\mathbf{r})}. \tag{1.46}$$

The ground-state energy functional in Eq. (1.40) can then be expressed as:

$$\begin{aligned} E_0[\rho(\mathbf{r})] &= 2\sum_{i=1}^{N/2} \left\langle \phi_i(\mathbf{r}) \left| -\frac{1}{2}\nabla^2 \right| \phi_i(\mathbf{r}) \right\rangle - \sum_{A=1}^{M} \int \frac{Z_A \rho(\mathbf{r}_1)}{r_{1A}} d\mathbf{r}_1 \\ &+ \frac{1}{2}\int\int \frac{\rho(\mathbf{r}_1)\rho(\mathbf{r}_2)}{r_{12}} d\mathbf{r}_1 d\mathbf{r}_2 + E_{XC}[\rho(\mathbf{r})]. \end{aligned} \tag{1.47}$$

If the exact form of the exchange-correlation energy $E_{XC}[\rho(\mathbf{r})]$ is known, then the exact ground-state energy and density of the system can be calculated readily. However, $E_{XC}[\rho(\mathbf{r})]$ is not known. $E_{XC}[\rho(\mathbf{r})]$ is usually approximated by separating it into two parts, pure exchange and pure correlation functionals

$$E_{XC}[\rho(\mathbf{r})] = E_X[\rho(\mathbf{r})] + E_C[\rho(\mathbf{r})] \tag{1.48}$$

and the approximation is done within the local density approximation (LDA), generalised-gradient approximation (GGA) or a hybrid of the two.

In the local density approximation, $E_{XC}[\rho(\mathbf{r})]$ is expressed as

$$E_{XC}^{LDA}[\rho(\mathbf{r})] = \int \varepsilon_{XC}[\rho(\mathbf{r})]\rho(\mathbf{r}) d\mathbf{r} \tag{1.49}$$

where $\varepsilon_{XC}[\rho(\mathbf{r})]$ is the exchange-correlation energy per particle (or energy density) of a homogeneous electron gas of density $\rho(\mathbf{r})$. The values of $\varepsilon_{XC}[\rho(\mathbf{r})]$ are based on Monte Carlo calculations by Ceperley and Alder[18] and interpolation procedures provided by Vosko, Wilk and Nusair (VWN)[19]. The term LDA in a more general case is called the *local spin density approximation* (LSDA). LSDA usually gives good results for systems with a fairly large homogeneous charge density $\rho(\mathbf{r})$. The main shortcoming of LSDA is when it is applied to a system with large inhomogeneity; it tends to overestimate electron correlation resulting in the over-binding of molecules, *i.e.*, too short bond lengths.

In order to improve the LSDA approach, $E_{XC}[\rho(\mathbf{r})]$ must not only depend on the electron density but also in its gradient, *i.e.*,

$$E_{XC}^{GGA}[\rho(\mathbf{r})] = \int \varepsilon_{XC}[\rho(\mathbf{r})]\rho(\mathbf{r})d\mathbf{r} + \int G_{XC}[\rho(\mathbf{r}), \nabla\rho(\mathbf{r})]d\mathbf{r} \qquad (1.50)$$

This *non-local* method is called the *gradient corrected* or *generalised-gradient approximation* (GGA). The functional G_{XC} usually provides corrections to the limitations of E_{XC} in LSDA. However, there is no universal formula for obtaining G_{XC}. A large number of density functionals are available in the literature including functionals due to Becke (B or B88[20], B95[21], B97[22]), Perdew and Wang (P86[23], PW86[24], PW91) and Lee, Yang and Parr (LYP[25]) to name a few.

Another method for formulating density functionals is by expressing the exchange-correlation energy by a suitable combination of LSDA, exact exchange and gradient correction terms. The resulting functional is often called a *hybrid functional.* An example is the *Becke 3-parameter functional*[26]:

$$E_{XC}^{B3} = E_{XC}^{LSDA} + a(E_X^{exact} - E_X^{LSDA}) + b\Delta E_X^B + c\Delta E_C^{GGA} \qquad (1.51)$$

where a, b, and c are *semiempirical coefficients* to be determined by an appropriate fit to experimental data, E_X^{exact} is the exact exchange energy, ΔE_X^B is Becke's correction to LSDA for exchange, and ΔE_C^{GGA} is the gradient correction for correlation. Commonly used hybrid functionals are the B3PW91 and B3LYP.

1.4 Pseudopotential Methods

In the methods described in the previous sections, all the electrons are explicitly treated and each occupied molecular orbitals is described by basis set with which the expansion coefficients have to be determined. The larger the system, the larger the basis needed to describe the molecular orbitals and the more expansion coefficients have to be found. From a computational point of view, an increase in the size of a chemical system under investigation translates into higher demands in computational resources, *e.g.*, CPU time, memory, disk space. However, using the fundamental chemical fact that most of the chemical properties of molecular systems are described by the interaction of valence electrons (while the low lying core electrons remain relatively chemically inert), performing calculations only on the valence electrons and replacing the interactions among the core electrons with some potential will lead to a large reduction of the basis set size, and lesser demand for computational resources. This basic idea was introduced by Hellman[27]. He proposed that the chemically inert electrons could be replaced by a suitable potential function called a *pseudopotential.* A detailed discussion on pseudopotential theory can be found in Ref. [28]

The aim of the pseudopotential method is to divide the total number of electrons into N_c core electrons and N_v valence electrons by constructing potentials which only depend on the coordinates of the N_v valence electrons and take into account the influence of the chemicaly inert N_c core electrons. In the pseudopotential method, the electronic hamiltonian for the N_v electrons is written as:

$$\hat{H}^{val} \equiv \hat{H}^{val}(1,2,\ldots,N_v) = \sum_{i=1}^{N_v} \hat{h}(i) + \sum_{i=1}^{N_v}\sum_{j>i}^{N_v} \frac{1}{r_{ij}}. \tag{1.52}$$

The one-electron hamiltonian operator $\hat{h}(i)$ is defined as:

$$\hat{h}(i) = -\frac{1}{2}\nabla_i^2 + \hat{V}_{core}^{PP} \tag{1.53}$$

where the first term represents the kinetic energy of the valence electrons and the second is the core potential operator. $\hat{V}_{core}^{PP}$ represents terms such as the potential energy of the valence electron i interacting with an effective nuclear charge (arising from the screening of the nucleus by N_c core electrons), a nonlocal term that models the Coulomb and exchange interactions between the core and valence electrons, and a projection operator. There are two types of pseudopotential methods in use, namely, the *model core potential* (MCP) and the *effective core potential* (ECP). Both methods try to model $\hat{V}_{core}^{PP}$ by using local potentials and by utilizing Gaussian-type functions with some adjustable parameters.

1.4.1 Model Core Potential

The model core potential method was proposed by Bonifacic and Huzinaga in mid-1970s[29, 30, 31, 32, 33] and was successfully tested in molecular calculations[34, 35, 36]. The MCP method was recently reviewed by Huzinaga[37, 38, 39]. In the MCP method, $\hat{V}_{core}^{PP}$ in Eq. (1.53) for each atomic center α is replaced by a potential representing the effect of effective nuclear charge $z_\alpha = Z - N_c$, the Coulombic and exchange interaction between the core and valence electrons, V_i^α, and a characteristic projection operator P_i^α, which ensures orthogonality of the valence orbitals to all core orbitals ϕ_c^α, *i.e.*,

$$\hat{V}^{MCP} = \frac{z_\alpha}{r_{i\alpha}} + \hat{V}_i^\alpha + \hat{P}_i^\alpha \tag{1.54}$$

In the MCP formalism, the one-electron hamiltonian $\hat{h}(i)$ becomes[40, 41]

$$\hat{h}(i) = -\frac{1}{2}\nabla_i^2 + \left(-\frac{z_\alpha}{r_{i\alpha}} + \hat{V}_i^\alpha + \hat{P}_i^\alpha\right). \tag{1.55}$$

$\hat{V}_i^\alpha$ is the spherically-symmetric local potential approximating the exact atomic non-local core potential,

$$V_i^\alpha = -\frac{z_\alpha}{r_{i\alpha}} \sum_k A_{k\alpha} r_{i\alpha}^{n_{k\alpha}} e^{-\zeta_{k\alpha} r_{i\alpha}^2} \tag{1.56}$$

where $n_{k\alpha}$ is 0 or 1 (see Ref. [42]) and the parameters $\{A_{k\alpha}, \zeta_{k\alpha}\}$ are specific for the atom α.

$\hat{P}_i^\alpha$ is the projection operator,

$$\hat{P}_i^\alpha = \sum_c B_c^\alpha |\phi_c^\alpha\rangle\langle\phi_c^\alpha|, \tag{1.57}$$

which shifts the core orbitals into the virtual space making it possible for the correct representation of the nodal structure of the valence orbitals. The shift parameter B_c^α is defined as:

$$B_c^\alpha = -f_c^\alpha \epsilon_c^\alpha, \tag{1.58}$$

ϵ_c^α being the core orbital energies. A fixed value of f_c^α is usually chosen making the MCP model depend only on $A_{k\alpha}$, and $\zeta_{k\alpha}$. The parameters $A_{k\alpha}$ and $\zeta_{k\alpha}$ are optimized by fitting the MCP orbital energies and shapes to reference atomic Hartree-Fock calculations. The fitting is done by minimizing the following function:

$$\delta = \sum_j \left[w_j^\epsilon \left|\epsilon_j^{ref} - \epsilon_j^{MCP}\right| + w_j^R \sum_k r_k^2 \left[R_j^{ref}(r_k) - R_j^{MCP}(r_k)\right]^2 \right] \tag{1.59}$$

where w_j are weight factors, ϵ_j are orbital energies, and R_j are radial functions defined over a grid r_k.

1.4.2 Effective Core Potentials

The effective core potential method is another pseudopotential method which is commonly used in computational studies. For reviews of the ECP method, see Refs. [43, 44, 45] and for a formal analysis of the ECP method, see the recent paper of Dyall[46]. In ECP, $\hat{V}_{core}^{PP}$ is represented by a semilocal pseudopotential

$$\hat{V}^{ECP} = U^{local} + \sum_l^{l_{max}} \left[U_l - U^{local}\right] P_l \tag{1.60}$$

where the l_{max} is the maximum angular momentum of the core orbitals. $\hat{V}^{ECP}$ is usually given in terms of Gaussian functions [47, 48] as:

$$\hat{V}^{ECP}_{core} = -\frac{z_\alpha}{r_i} + \sum_l \sum_k A_{kl} e^{-\zeta_{kl} r_i^2} P_l \qquad (1.61)$$

where z_α denotes the charge of the core on atom α, and A_{kl} and ζ_{kl} are adjustable parameters of the model. The P_l represents the projection operator onto the angular momentum l and is defined as:

$$P_l = \sum_{m=-l}^{l} |Y_{lm}\rangle \langle Y_{lm}| \qquad (1.62)$$

where Y_{lm} is the usual spherical harmonic function. Using a semilocal representation eliminates the necessity for projection onto specific orbitals and allows for the selection of the pseudopotential of the appropriate angular symmetry.

The parameters A_{kl} and ζ_{kl} in the Gaussian expansion of the radial potential are determined by fitting to either atomic all-electron HF calculation or excitation energies.

1.4.3 Comparison of MCP and ECP models

Pseudopotential methods offer large computational savings over their all-electron counterparts due to the reduction of the number of electrons explicitly treated in the calculations without compromising too much the accuracy of the results[45]. In performing all-electron calculations, all radial nodal structures of orbitals naturally arise. In the development of MCP, these radial nodal structures are preserved via the projection operator. In the ECP approach, however, the valence atomic orbitals are converted to nodeless pseudo-orbitals. This is accomplished by fitting to the radial function of the reference orbital at a large distance from the nucleus. Although the valence region is well represented, the region close to the nucleus is not.

The retention of the correct nodal structure in the MCP approach is an advantage over their ECP counterpart. This was shown to be very important in the study of properties that involve electrons near the nucleus, like spin-orbit coupling constants calculations[49] and atomic correlation energies[50]. However, in terms of computational speed, particularly in the evaluation of two-electron integrals, ECPs perform faster. This is because fewer basis functions are needed to represent the nodeless radial function as compared to MCP.

1.4.4 Relativistic Pseudopotentials

Real chemical systems intrinsically incorporate relativistic effects. As the electron moves at a significant speed comparable to the speed of light, its mass increases. The resulting increase in the centrifugal force causes the s and p orbitals to contract closer to the nucleus. This contraction creates an extra shielding of the nucleus causing the higher angular momentum orbitals d and f to expand (indirect relativistic effect). The balance between the degree of orbital contraction and expansion will dictate the appropriate bond lengths in molecular systems. Another main effect caused by relativity is spin-orbit interaction. *Spin-orbit effects* result in the splitting of states in an atom.

To computationally describe chemical systems accurately, especially those which involve heavy atoms, relativistic effects must also be included in the calculation. For lighter nuclei, relativistic effects can be considered negligible. However, for heavier nuclei, relativistic effects become significantly important and must not be neglected. For a review on the theory of relativistic effects as applied to electronic structure calculations, see Ref. [51]

Some portion of the relativistic effects can be indirectly incorporated into pseudopotential methods. In generating a relativistic pseudopotential, the pseudopotential parameters are determined via the same fitting procedure described above. However, instead of doing non-relativistic HF calculation to obtain the reference atomic orbitals and orbital energies, a modified HF model to include relativistic effects is often used. This approach is called *quasirelativistic Hartree-Fock*. The Cowan-Griffin relativistic HF equation[52] is often used to generate the reference quasirelativistic atomic orbitals and orbital energies[40] which would then be incorporated in the MCP or ECP core potentials.

1.5 Basis Sets

The solution to the wave functional and density functional method requires the use of spatial orbitals ϕ_i expanded as a linear combination of a set of one-electron basis functions,

$$\phi_i(\mathbf{r}) = \sum_{\alpha} \chi_\alpha(\mathbf{r} - \mathbf{R}_\alpha) c_{\alpha i}.$$

The use of a complete set of basis functions results in an exact solution. In practice, however, this is not possible because of the limitation in computer resources available. Instead, a finite set of basis functions is used. Basis sets must be properly chosen if accurate molecular results are desired. In choosing basis functions, one has to consider two basic requirements: first, the function must correctly describe the qualitative description of the orbitals, *i.e.*, it must exhibit correct asymptotic behaviour as $r \to 0$ and must not decay too rapidly at $r \to \infty$ and second, it should be relatively easy to evaluate computationally. There are two types of basis functions currently employed in molecular calculations, namely, *Slater-type functions* (STF) and *Gaussian-type functions* (GTF). The former satisfies the first requirement while the latter satisfies the second as we shall see later. This section discusses a brief introduction to basis functions and some of the terms and notation associated with them. For a more detailed and thorough reviews on basis sets, see Refs. [53, 54, 55].

1.5.1 Slater and Gaussian Type Functions

The basis function χ is normally expressed in spherical coordinates as

$$\chi(\zeta, n, l, m; r, \theta, \phi) = R_{nl}(\zeta; r)Y_{lm}(\theta, \phi) \tag{1.63}$$

where $R_{nl}(r)$ is the radial distribution function and $Y_{lm}(\theta, \phi)$ is the spherical harmonic function describing the shape of the orbital. The labels n, l and m are the principal, angular momentum and magnetic quantum numbers, respectively.

The Slater-type functions were initially used in atomic and molecular calculations due to their similarity to the atomic orbitals of the hydrogen atom. They are described in spherical coordinates as[53]:

$$\chi(\zeta, n, l, m; r, \theta, \phi) = Nr^{n-1}e^{-\zeta r}Y_{lm}(\theta, \phi) \tag{1.64}$$

$$N = (2\zeta)^{n+\frac{1}{2}}[(2n)!]^{-\frac{1}{2}} \tag{1.65}$$

where N is the normalization constant and ζ is the exponent that determines the extent of the radial function. Although STF has the correct behavior at $r \to 0$ and at $r \to \infty$, the function is not good enough for fast evaluation of the two-electron integrals. GTFs offer a solution. GTFs are described in two different forms - in spherical and in Cartesian coordinates[53]. The spherical Gaussian form is expressed as

$$\chi(\zeta, n, l, m; r, \theta, \phi) = Nr^{n-1}e^{-\zeta r^2}Y_{lm}(\theta, \phi) \tag{1.66}$$

$$N = 2^{n+1}[(2n-1)!!]^{-\frac{1}{2}}(2\pi)^{-\frac{1}{4}}\zeta^{\frac{(2n+1)}{2}}$$

$$n = l+1, l+3, l+5, \ldots \tag{1.67}$$

The GTF in Cartesian Gaussian form, on the other hand, is

$$\chi(\zeta, l, m, n; x, y, z) = Ne^{-\zeta r^2}x^l y^m z^n \tag{1.68}$$

$$N = (2\pi)^{\frac{3}{4}}[(2l-1)!!(2m-1)!!(2n-1)!!]^{-\frac{1}{2}}\zeta^{\frac{[l+m+n+\frac{3}{4}]}{2}} \tag{1.69}$$

where N is the normalization constant, x, y and z are Cartesian coordinates, and l, m and n are just integer exponents not to be mistaken for quantum numbers. Normally, the sum of l, m and n is defined as L, (*i.e.*, $L = x + y + z$) and is associated with the shape of the orbitals. $L = 0$ corresponds to s-type function, $L = 1$ to p-type functions, $L = 2$ to d-type functions, and so on[55]. In both forms of the GTF, ζ represents the orbital exponents. Although a GTF exhibits a zero slope instead of a cusp as $r \to 0$ and decays too fast as $r \to \infty$, evaluation of the two-electron integrals is rather fast and easy to implement computationally. Though a single GTF does not properly describe the orbital as the STF does, by combining a reasonable number of GTFs with different exponents and coeficients, an approximation to the shape of STF can be obtained. However, combining a large number of GTFs also increases computational demands. The solution is to form linear combination of GTF (from now on refered to as *primitive GTFs*) with coefficients that are not allowed to change during the SCF procedure[1, 53]:

$$\chi_{\mu,L}^{cGTF} = \sum_{i=1}^{K} d_{\mu,i}^{L} \chi_{L}^{pGTF}(\zeta_i; r) \tag{1.70}$$

where $\chi_{\mu,L}^{cGTF}$ are called *contracted GTFs* (cGTFs), $d_{\mu,i}^{L}$ are refered to as contraction coefficients and L refers to the type of "orbital shapes" described above. $\chi_{\mu,L}^{cGTF}$ determines the number of basis function that is used in molecular calculations.

There are two schemes for making contracted basis sets, namely, *segmented* and *general*. However, it is not the intent of this thesis to discuss in great detail the different terms and numerous notations found in the literature. Only a general discussion is presented. In the segmented contraction scheme, a given set of pGTFs is grouped into smaller sets of functions in which the number of primitives and contractions are explicitly specified and is given in the order of increasing angular momentum quantum number. For example, (742111,5311,11) or (742111/5311/11) means that there are 6 s-type basis functions consisting of 7, 4, 2, 1, 1, and 1 primitives, respectively; 4 p-type basis functions consisting of 5, 3, 1 and 1 primitives, respectively; and the d-type basis function has 2 uncontracted primitives, respectively. In the general contraction scheme, the same Gaussian primitives of a given angular momentum appear in all the contracted functions having the angular momentum, but with different contraction coefficient. This form has been introduced by Raffenetti in 1973[56].

There are several ways of obtaining the best expansion $\chi_{\mu,L}^{cGTF}$. One approach is by varying $d_{\mu,i}^{L}$ and the exponents ζ_i until the lowest total HF energy of the atom is attained. Sometimes the exponents are functionally related to each other: an example of this is the well-tempered basis set.

1.5.2 Well-tempered, MCP, and ECP Basis Sets

The *well-tempered gaussian basis set* (WTBS) was introduced by Huzinaga, Klobukowski, and Tatewaki[57]. In the WTBS expansion, the N total number of exponents ζ are generated by the following formula

$$\begin{aligned} \zeta_0 &= \alpha, \qquad \zeta_1 = \alpha\beta \\ \zeta_k &= \zeta_{k-1}\beta\left[1+\gamma\left(\frac{k}{N}\right)^{\delta}\right], \qquad k = 2, \ldots, N \end{aligned} \tag{1.71}$$

where the parameters α, β, γ and δ, common for the radial functions of all angular symmetries, were optimized by minimizing the ground-state energy of an atom. The Gaussian primitives of the WTBS share exponents between

$s-$, $p-$, $d-$, and $f-$type orbital functions. The WTBS is a large basis set designed for accurate all-electron calculation.

Due to tremendous savings in computational cost offered by pseudopotential methods, various pseudopotential basis sets were also developed. Large- and small-core pseudopotentials as well as quasirelativistic pseudopotential basis sets have been published. For the atoms from the main-group, a *large-core* pseudopotential comprise the outermost ns and np shells and a *small-core* pseudopotential also includes the (n-1)d shell in the valence space.

In the MCP model, the basis set is often tabulated as parameters of the expression given in Eq. (1.56) for optimized sets of $\{A_{k\alpha}, \zeta_{k\alpha}\}$, and Eq. (1.57) for the shift parameter B_c and core orbitals. MCP non-relativistic and quasi-relativistic parameters are available for most of the elements of the periodic table[58, 59, 60] and were calibrated and benchmarked for use in molecular calculations[61, 62]. The MCP parameters and valence basis sets have been incorporated in the CADPAC[63] suite of programs and the developmental version of the GAMESS-US[64, 65] program.

In the ECP model, the basis sets are usually tabulated as parameters of the Gaussian expression:

$$U^{ECP}(r) = \sum_{i=1}^{M} A_i r^{n_i} e^{-\zeta_i r^2} \tag{1.72}$$

where r is the distance from the nucleus raised to power n_i, and A_i and ζ_i are sets of optimized ECP parameters. There are different ECP basis sets available in the literature. Among these ECPs were due to Hay and Wadt[66, 67, 68] and Stevens, Basch, Krauss, Jasien and Cundari(SBKJC)[69, 70, 71], also known as the *compact effective core potentials.* These two ECPs are part of the official release of Gaussian[72] and GAMESS-US programs. ECPs due to Ermler, Ross and Christiansen[73, 74, 75, 76, 77, 78, 79] have been published for all the elements of the periodic table. ECPs due to Dolg, Stoll and Preuss[80, 81, 82, 83, 84, 85, 86, 87, 88, 89] have been successfully tested and incorporated in TURBOMOLE[90] and Molpro[91] suite of quantum chemistry programs. Other relativistic ECP (RECP) parameters[92, 93, 94, 95] have been published and successfully used in molecular calculations.

Chapter 2

The Development of the Well-tempered Model Core Potentials

The model core potential is a valence *ab initio* method that can be used for the prediction and rationalization of experimental results without resorting to expensive all-electron calculations and without the need for empirical adjustment, characteristic of semi-empirical approaches. The model is capable of fully representing the correct nodal structures of valence orbitals. The MCP valence basis sets and associated parameters that have been published[58, 59, 60] were developed by using a small number of pGTFs in which the exponents are optimized via a fitting procedure using the solution to the numerical atomic Hartree-Fock equations as the reference function[40]. The number of nodes included to represent the valence orbitals depended on the number of pGTF used for their analytical representation.

The analytic form of the Hartree-Fock model is a system of integrodifferential equations, *i.e*,

$$\left\{-\frac{1}{2}\frac{d^2}{dr^2}+\frac{l(l+1)}{2r^2}-\frac{Z}{r}+\hat{v}_{nl}^{HF}(r)\right\}R_{nl}(r)$$
$$=\epsilon_{nl}R_{nl}(r)+\sum_{n'}\sum_{l}\epsilon_{nl,n'l}R_{nl,n'l}(r) \qquad (2.1)$$

where $\hat{v}_{nl}^{HF}(r)$ is the usual nonlocal HF potential introduced in Eq. (1.18) consisting of the Coulomb and exchange integrals. The numerical HF method is based on the finite difference approximation where the radial function $R_{nl}(r)$ in Eq. (2.1) is approximated at a discrete set of grid points r_j. The differential and integral operators involved in the analytic HF equations are replaced by their finite difference counterparts.

One of the most successful implementations of the nonrelativistic numerical HF method for the atoms was incorporated in the multiconfiguration Hartree-Fock (MCHF) program developed by Froese Fischer[96, 97, 98]. The MCHF represents the wavefunction as a linear combination of configurational state functions(CSFs) $\Phi(\gamma LS)$:

$$\Psi^{MCHF}(\gamma LS) = \sum_{i=1}^{m} c_i \Phi(\gamma_i LS), \tag{2.2}$$

as the truncated form of Eq. (1.35). In Eq. (2.2), both the expansion coefficients c_i and the CSF Φ_i are optimized. The approximation using this linear combination of determinants is done in order to recover the electron correlation absent in the pure HF method. For the details on the numerical MCHF procedures and results, see Ref. [98].

Relativistic effects are incorporated in the MCPs via the Cowan-Griffin[52] relativistic modification of the HF equations given by Eq. (2.1). This is accomplished by adding to Eq. (2.1) the *mass-velocity*, $\hat{v}_{nl}^{MV}(r)$ and *Darwin*, $\hat{v}_{nl}^{D}(r)$ potential operators[40]:

$$\left\{-\frac{1}{2}\frac{d^2}{dr^2} + \frac{l(l+1)}{2r^2} - \frac{Z}{r} + \hat{v}_{nl}^{HF}(r) + \hat{v}_{nl}^{MV}(r) + \hat{v}_{nl}^{D}(r)\right\} R_{nl}^{qr}(r)$$
$$= \epsilon_{nl}^{qr} R_{nl}^{qr}(r) + \sum_{n'} \sum_{l} \epsilon_{nl,n'l}^{qr} R_{nl,n'l}^{qr}(r) \tag{2.3}$$

where

$$\hat{v}_{nl}^{MV}(r) = -\frac{\alpha^2}{2}\left[\epsilon_{nl,n'l}^{qr} - \bar{v}_{nl}(r)\right]^2 \tag{2.4}$$

and

$$\hat{v}_{nl}^{D}(r) = -\delta_{l0}\frac{\alpha^2/4}{1+\alpha^2\left[\epsilon_{nl}^{qr} - \bar{v}_{nl}(r)\right]/2}\frac{d\bar{v}_{nl}(r)}{dr}\left(\frac{d}{dr} - \frac{1}{r}\right) \tag{2.5}$$

The operator $\bar{v}_{nl}(r)$ is Cowan's local approximation to the non-local Hartree-Fock potential $\hat{v}_{nl}^{HF}$ and α is the fine structure constant. Numerically solving Eq. (2.3) and using its solutions (ϵ_{nl}^{qr} - the orbital energies and $R_{nl}^{qr}(r)$ - the radial functions) as reference for determining the MCP parameters leads to *quasirelativistic MCPs.*

In this thesis, a new family of MCPs were developed in a different approach. Instead of using numerical reference functions, the development proceeded by using analytical reference functions expanded in terms of a very large all-electron basis set. The well-tempered basis set(WTBS)[57, 99] was chosen for this thesis. The WTBS is an all-electron basis set designed to give results that are extremely close to the Hartree-Fock limit. Since WTBS can provide high quality results, by developing MCP valence basis sets based on the WTBS, the same quality of results is expected in the resulting new MCPs. These new MCPs have been called the *well-tempered model core potentials* (wtMCP) to emphasize their well-tempered origin. The details of the development of wtMCPs and some atomic results obtained from using the wtMCPs are the subjects of the rest of this chapter.

2.1 The Analytical Reference Functions

The nonrelativistic analytical reference functions are generated by solving the system of HF equations described in the previous chapter. The relativistic analytical reference functions, on the other hand, are usually made by using the analytic solution to the Dirac-Hartree-Fock(DHF) equation and its approximations.

The DHF method uses the four-component Dirac wavefunction[100, 101]

$$\Psi = \begin{pmatrix} \phi \\ \chi \end{pmatrix} \tag{2.6}$$

where ϕ and χ represent the large- and small-components of the wavefunction, respectively. The Dirac equations is written as two coupled equations in ϕ and χ

$$\begin{aligned} (V-E)\phi + c(\vec{\sigma}\cdot\vec{p})\chi &= 0 \\ c(\vec{\sigma}\cdot\vec{p}\phi) + (V-E-2mc^2)\chi &= 0. \end{aligned} \tag{2.7}$$

where V is the scalar potential, $\vec{\sigma}$ represents the Pauli spin matrices, $\vec{p}$ is the momentum operator, and c is the speed of light. These coupled equations can be solved in terms of the large-component ϕ to give

$$\left[V + (\vec{\sigma}\cdot\vec{p})\frac{c^2}{2mc^2-(V-E)}(\vec{\sigma}\cdot\vec{p})\right]\phi = E\phi. \tag{2.8}$$

The presence of the potential V and energy E in the denominator of Eq. (2.8) makes it extremely difficult to solve. Several schemes have been proposed to simplify Eq. (2.8) by introducing approximations. Among these are the *zeroth-order regular approximation* (ZORA)[102, 103] method, the *Douglas-Kroll*(DK)[104] method developed by Hess[105, 106, 107], the relativistic approximation method developed by Dyall[108] and the *relativistic elimination of small components* (RESC)[109, 110] method developed by Nakajima and Hirao. In this thesis the RESC method is used to generate reference atomic orbitals. The RESC formulas presented here were described in full detail in the paper by Nakajima and Hirao[109].

In their development of the RESC scheme, Nakajima and Hirao proposed to replace the $(E-V)$ term in the denominator by the classical relativistic kinetic energy, T:

$$T = \sqrt{m^2c^4 + p^2c^2} - mc^2 \tag{2.9}$$

The resulting RESC Hamiltonian, $\hat{H}^{RESC}$ is expressed as

$$\begin{aligned} \hat{H}^{RESC} = \hat{T} &+ \hat{O}\hat{Q}\vec{p}V\vec{p}\hat{Q}\hat{O}^{-1} \\ &+ 2mc\hat{O}\hat{Q}^{1/2}V\hat{Q}^{1/2}\hat{O}^{-1} + i\hat{O}\hat{Q}\vec{\sigma}(\vec{p}V)\vec{p}\hat{Q}\hat{O}^{-1} \end{aligned} \tag{2.10}$$

where the operators $\hat{O}$ and $\hat{Q}$ are defined as

$$\hat{O} = \frac{1}{E_p + mc^2}\left[1 + \frac{p^2c^2}{(E_p + mc^2)^2}\right]^{1/2} \tag{2.11}$$

and

$$\hat{Q} = \frac{c}{E_p + mc^2} \tag{2.12}$$

with the energy of the electron given as

$$E_p = \sqrt{m^2c^4 + p^2c^2} \tag{2.13}$$

The RESC method with analytic gradients[110] has been recently implemented in the GAMESS-US[64, 65] computer program and is utilized in generating analytical reference functions in this thesis.

The nonrelativistic and scalar-relativistic analytical reference functions were prepared for each of the main-group atoms from Li to Rn by using fully uncontracted WTBS within the GAMESS-US program. Calculations were done for the lowest state of the ground-state electronic configuration of each atom. These provided both the analytical core functions for the projection operator of Eq. (1.57) as well as the analytical valence reference functions necessary for the optimization of MCP parameters via fitting procedure.

2.2 The wtMCP Valence Basis Sets

In preparing the wtMCP valence basis sets for optimization, the following procedure was followed. For the $s-$block elements, the original WTBS primitive Gaussian functions were used for the s and p valence orbitals. For the $p-$block elements, the original WTBS primitive Gaussian functions were used for the p and d valence orbitals while for the s orbitals, the Gaussian functions with the largest exponents were dropped. The omission of the largest exponents in the s space leads to identical number of Gaussian primitives used for both the s and p spaces. In both cases, the original WTBS primitive Gaussian functions were uncontracted at their free atom values.

The well-tempered basis functions share Gaussian exponents between the $s-$ and $p-$type functions. Such a selection of basis functions for the MCP valence basis set is an advantage - due to computational savings in the molecular integral evaluation provided that the integral code is able to utilize the shell structure of the sp basis functions. Although the wtMCP valence basis sets possess large Gaussian expansions, it affects only the one- and two-electron integral evaluation steps and no additional computational cost is incurred during the post-HF steps.

The wtMCP valence basis sets and the corresponding pseudopotentials were developed for the main-group elements. Nonrelativistic wtMCPs were developed for elements from Li to Rn while scalar-relativistic wtMCPs were developed for elements K to Rn. Table 2.1 shows the comparison of pGTF between AE and wtMCP valence basis sets for the main-group elements.

2.3 The Optimization Method

Function minimization is one of the most common problems encountered in computational research and is generally classified into two major classes – *gradient* and *non-gradient* techniques. Gradient techniques, in general, are efficient methods of locating the minimum of a function f but require the knowledge of at least the first derivative of the function with respect to all variables, x_i. However, when the first derivative of the function is very difficult to solve or even unknown (which is often the case), function minimization often resorts to non-gradient techniques.

Non-gradient methods minimize the function f along a set of directions. Although non-gradient methods are not as efficient as gradient methods, they may be designed to possess quadratic convergence, *i.e.*, to quickly converge to the minimum of the quadratic function. Such methods include that of Powell[111], which was later modified by Brent[112].

The basic idea of the Powell's method is to continuously update a set of linearly independent direction vectors $\mathbf{d}_1, \mathbf{d}_2, \ldots, \mathbf{d}_n$, by starting with an initial approximation to the minimum, $\mathbf{x}_0$, until all the directions are mutually conjugate after n iterations. The following outlines one iteration of Powell's basic algorithm[111, 112]:

1. For $i = 1, 2, \ldots, n$, calculate λ_i to minimize the function $f = f(\mathbf{x}_{i-1} + \lambda_i \mathbf{d}_i)$, and then set $\mathbf{x}_i = \mathbf{x}_{i-1} + \lambda_i \mathbf{d}_i$
2. For $i = 1, 2, \ldots, n-1$, set $\mathbf{d}_i = \mathbf{d}_{i+1}$
3. Set $\mathbf{d}_n = \mathbf{x}_n - \mathbf{x}_0$
4. Calculate λ to minimize the function $f = f(\mathbf{x}_0 + \lambda \mathbf{d}_n)$, and then set $\mathbf{x}_0 = \mathbf{x}_0 + \lambda \mathbf{d}_n$

Powell's method works very well as long as $\lambda_i \neq 0$. If, however, one of the $\lambda_i = 0$, the corresponding direction vector $\mathbf{d}_i$ will vanish. This results in the directions $\mathbf{d}_1, \mathbf{d}_2, \ldots, \mathbf{d}_n$ becoming linearly dependent and the correct minimum of the function may never be found since the direction set no longer span the entire parameter space. This problem of linear dependency was fixed by Brent by modifying Powell's algorithm such that the direction matrix $D = [\mathbf{d}_1, \mathbf{d}_2, \ldots, \mathbf{d}_n]$ was replaced by principal axes of the quadratic function, *i.e.*, an orthogonal matrix $Q = [\mathbf{q}_1, \mathbf{q}_2, \ldots, \mathbf{q}_n]$, where $\mathbf{q}_1, \mathbf{q}_2, \ldots, \mathbf{q}_n$ are the principal vectors. Other modifications made by Brent were the inclusion of an option for automatic scaling of the independent variables, and incorporating random step procedures to avoid premature termination in the computation of

Table 2.1: Comparison of pGTF between AE and wtMCP valence basis sets.

Atoms	AE			wtMCP	
	AO_{core}	$AO_{valence}$	pGTF	$AO_{valence}$	pGTF
Li - Be	1s	2s	20*s*	2s	20*s*
Na - Mg	1s 2s	3s	23*s*	3s	23*s*
		2p	13*p*	2p	13*p*
K - Ca	1s 2s 3s	4s	26*s*	4s	26*s*
	2p	3p	16*p*	3p	16*p*
Rb - Sr	1s 2s 3s 4s	5s	28*s*	5s	28*s*
	2p 3p	4p	20*p*	4p	20*p*
	3d		14*d*		
Cs - Ba	1s 2s 3s 4s 5s	6s	30*s*	6s	28*s*
	2p 3p 4p	5p	20*p*	5p	23*p*
	3d 4d		17*d*		
B - Ne	1s	2s	20*s*	2s	13*s*
		2p	13*p*	2p	13*p*
Al - Ar	1s 2s	3s	23*s*	3s	16*s*
	2p	3p	16*p*	3p	16*p*
Ga - Kr	1s 2s 3s	4s	26*s*	4s	20*s*
	2p 3p	4p	20*p*	4p	20*p*
		3d	14*d*	3d	14*d*
In - Xe	1s 2s 3s 4s	5s	28*s*	5s	23*s*
	2p 3p 4p	5p	23*p*	5p	23*p*
	3d	4d	17*d*	4d	17*d*
Tl - Rn	1s 2s 3s 4s 5s	6s	28*s*	6s	24*s*
	2p 3p 4p 5p	6p	24*p*	6p	24*p*
	3d 4d	5d	18*d*	5d	18d
	4f				

the function f. These modifications are discussed in great detail in the book by Brent[112]. In this work, the Brent's modification of the Powell algorithm was used for optimizing the wtMCP parameters.

For a closed-shell system, the MCP-HF equation is given by:

$$\hat{F}^{MCP}(i)\,|\phi_j(i)\,\rangle = \epsilon_j|\,\phi_j(i)\,\rangle\,. \tag{2.14}$$

The MCP-HF operator $\hat{F}^{MCP}(i)$ is defined as

$$\hat{F}^{MCP}(i) = \hat{h}(i) + \sum_j \left(2\hat{J}[\phi_j] - \hat{K}[\phi_j]\right) \tag{2.15}$$

where $\hat{h}(i)$ is the one-electron Hamiltonian operator given by Eq. (1.55). Since $\hat{F}^{MCP}(i)$ depends on $\hat{h}(i)$, the solutions of the MCP-HF equations that give rise to MCP radial functions R_j^{MCP} and MCP orbital energies ϵ_j^{MCP} will naturally depend on the parameters A_k, ζ_k (Eq. (1.56)) and B_c (Eq. (1.57)), *i.e.*,

$$R_j^{MCP} = R_j^{MCP}(\{A_k\},\{\zeta_k\},\{B_c\}) \tag{2.16}$$

$$\epsilon_j^{MCP} = \epsilon_j^{MCP}(\{A_k\},\{\zeta_k\},\{B_c\}). \tag{2.17}$$

In order to reduce the number of MCP parameters to be optimized, the shift parameter B_c was fixed to twice the value of the reference core orbital energies ϵ_c, *i.e.*,

$$B_c = -2\epsilon_c. \tag{2.18}$$

This leads R_j^{MCP} and ϵ_j^{MCP} to depend only on the parameters A_k and ζ_k.

Using the Brent's optimization program, the optimized values A_k and ζ_k are determined via fitting procedure by minimizing the function given by Eq. (1.59):

$$\delta = \sum_j \left[w_j^{\epsilon} \left|\epsilon_j^{ref} - \epsilon_j^{MCP}\right| + w_j^{R} \sum_k r_k^2 \left[R_j^{ref}(r_k) - R_j^{MCP}(r_k)\right]^2 \right]$$

The optimized wtMCP parameters and the corresponding basis sets for the main-group elements have been tabulated[113, 114].

2.4 The Quality of the wtMCP

The newly developed wtMCP valence basis sets and the corresponding pseudopotentials are tested in atomic calculations in order to assess their quality. In the optimization and fitting procedure described above, the fits of the wtMCP radial functions against the reference radial functions are excellent. Figures 2.1–2.3 show the radial distribution functions for Xe(^{1}S) comparing the $5s-$, $5p-$ and $4d-$type functions between the nonrelativistic wtMCP and the Hartree-Fock reference orbitals. Similar quality of fits is also obtained between the scalar-relativistic wtMCP and the RESC reference functions as

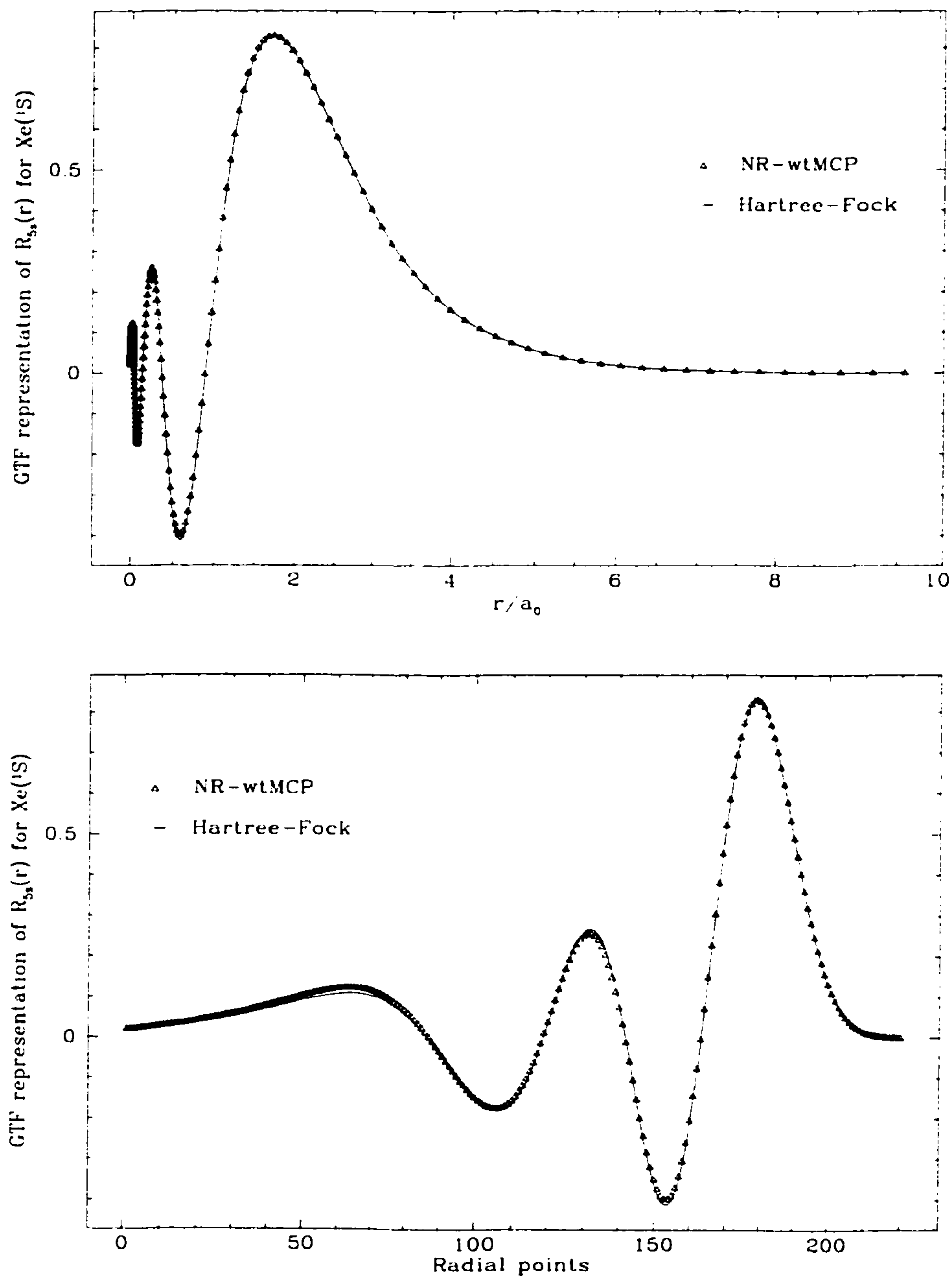

Figure 2.1: Non-relativistic Xe(^{1}S) 5s radial distribution function.

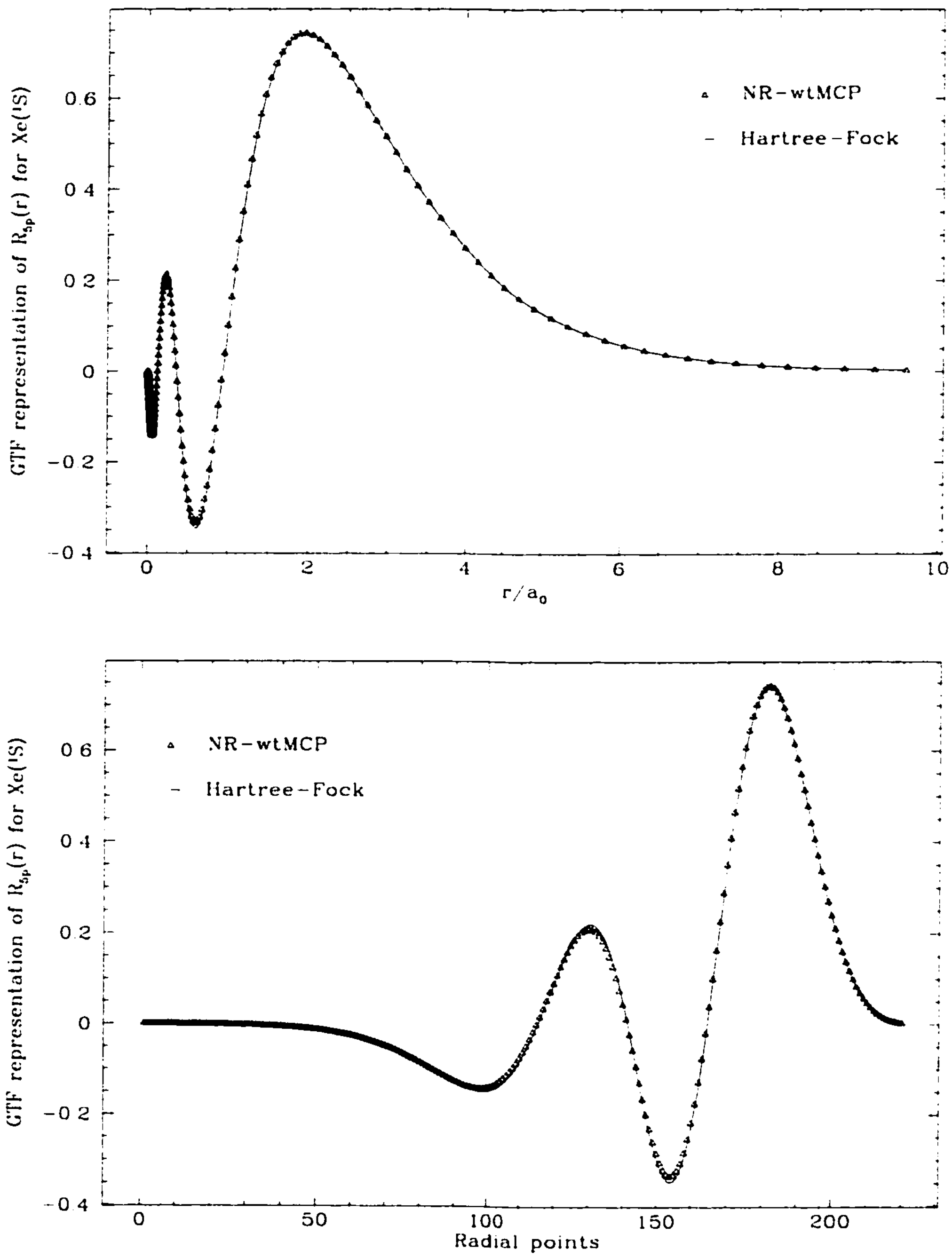

Figure 2.2: Non-relativistic Xe(^{1}S) $5p$ radial distribution function.

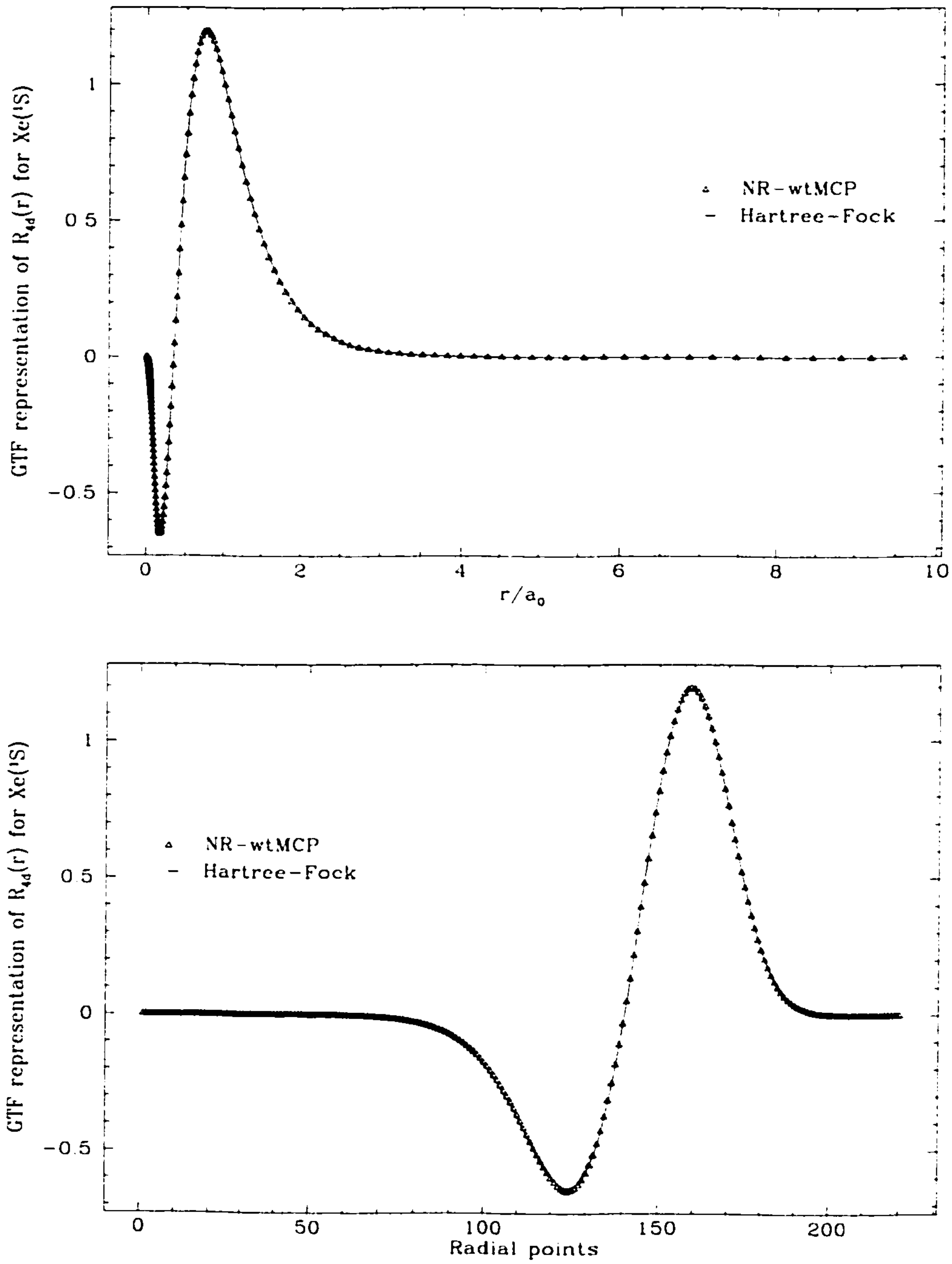

Figure 2.3: Non-relativistic Xe(^{1}S) $4d$ radial distribution function.

shown in Figures B.1–B.3. Excellent agreement is also obtained between the reference and wtMCP orbital energies with energy differences smaller than 1 μE_h.

The expectation values $\left\langle r^k \right\rangle$ defined as

$$\left\langle r^k \right\rangle = \left\langle R_{nl} \left| r^k \right| R_{nl} \right\rangle, \tag{2.19}$$

which are important in describing atomic and molecular properties such as dipole moment, quadrupole moments, *etc.*, are also compared between the reference and wtMCP basis sets. Table 2.2 compares the values of $\left\langle r^k \right\rangle$ between the reference and wtMCP for the noble-gas atoms. Typically, the difference in $\left\langle r^k \right\rangle$ are less than 1%. However, larger deviations are seen for the $\langle r^{-2} \rangle$ values for the s−type orbitals due to the absence of the highest exponents in the s basis set.

Table 2.2: Radial expectation values for noble-gas atoms.

Atom	**nl**	$\left\langle r^k \right\rangle$	**HF**	**NR-wtMCP**	**RESC**	**SR-wtMCP**
Ne	$2s$	$\langle r^1 \rangle$	0.8921	0.8918		
		$\langle r^2 \rangle$	0.9671	0.9662		
		$\langle r^{-1} \rangle$	1.6326	1.6214		
		$\langle r^{-2} \rangle$	11.0713	10.5389		
	$2p$	$\langle r^1 \rangle$	0.9653	0.9649		
		$\langle r^2 \rangle$	1.2284	1.2277		
		$\langle r^{-1} \rangle$	1.4354	1.4364		
		$\langle r^{-2} \rangle$	3.0588	3.0669		
Ar	$3s$	$\langle r^1 \rangle$	1.4222	1.4183		
		$\langle r^2 \rangle$	2.3504	2.3392		
		$\langle r^{-1} \rangle$	0.9620	0.9636		
		$\langle r^{-2} \rangle$	5.4144	5.2397		
	$3p$	$\langle r^1 \rangle$	1.6629	1.6582		
		$\langle r^2 \rangle$	3.3105	3.2946		
		$\langle r^{-1} \rangle$	0.8141	0.8173		
		$\langle r^{-2} \rangle$	1.4736	1.4899		

continued on next page

Table 2.2: *continued*

Atom	nl	$\langle r^k \rangle$	HF	NR-wtMCP	RESC	SR-wtMCP
Kr	$4s$	$\langle r^1 \rangle$	1.6294	1.6252	1.6004	1.5963
		$\langle r^2 \rangle$	3.0404	3.0246	2.9352	2.9208
		$\langle r^{-1} \rangle$	0.8042	0.8046	0.8247	0.8231
		$\langle r^{-2} \rangle$	4.6037	4.4874	6.1517	4.9039
	$4p$	$\langle r^1 \rangle$	1.9515	1.9461	1.9441	1.9392
		$\langle r^2 \rangle$	4.4542	4.4305	4.4242	4.4034
		$\langle r^{-1} \rangle$	0.6692	0.6704	0.6735	0.6742
		$\langle r^{-2} \rangle$	1.2388	1.2596	1.2843	1.2784
	$3d$	$\langle r^1 \rangle$	0.5509	0.5506	0.5528	0.5511
		$\langle r^2 \rangle$	0.3715	0.3702	0.3745	0.3711
		$\langle r^{-1} \rangle$	2.2769	2.2761	2.2726	2.2744
		$\langle r^{-2} \rangle$	6.7083	6.7169	6.6959	6.7074
Xe	$5s$	$\langle r^1 \rangle$	1.9810	1.9806	1.9054	1.9018
		$\langle r^2 \rangle$	4.4401	4.4322	4.1135	4.0959
		$\langle r^{-1} \rangle$	0.6479	0.6478	0.6826	0.6878
		$\langle r^{-2} \rangle$	3.5068	4.1210	6.6436	5.6358
	$5p$	$\langle r^1 \rangle$	2.3380	2.3363	2.3145	2.3094
		$\langle r^2 \rangle$	6.2767	6.2601	6.1616	6.1323
		$\langle r^{-1} \rangle$	0.5472	0.5427	0.5556	0.5556
		$\langle r^{-2} \rangle$	0.9707	0.9447	1.0688	1.0958
	$4d$	$\langle r^1 \rangle$	0.8704	0.8673	0.8762	0.8750
		$\langle r^2 \rangle$	0.8808	0.8731	0.8941	0.8891
		$\langle r^{-1} \rangle$	1.5087	1.5107	1.5035	1.4965
		$\langle r^{-2} \rangle$	4.0991	4.0787	4.1092	4.0136

continued on next page

Table 2.2: *continued*

Atom	nl	$\langle r^k \rangle$	HF	NR-wtMCP	RESC	SR-wtMCP
Rn	6*s*	$\langle r^1 \rangle$	2.1566	2.1507	1.9405	1.9342
		$\langle r^2 \rangle$	5.2327	5.2036	4.2502	2.2240
		$\langle r^{-1} \rangle$	0.5855	0.5852	0.6701	0.6677
		$\langle r^{-2} \rangle$	3.2008	2.9740	15.6259	6.2336
	6*p*	$\langle r^1 \rangle$	2.5434	2.5364	2.4598	2.4528
		$\langle r^2 \rangle$	7.3698	7.3288	6.9232	6.8844
		$\langle r^{-1} \rangle$	0.4953	0.4944	0.5187	0.5174
		$\langle r^{-2} \rangle$	0.8882	0.8558	1.2150	1.0864
	5*d*	$\langle r^1 \rangle$	1.0605	1.0514	1.0751	1.0650
		$\langle r^2 \rangle$	1.2813	1.2579	1.3222	1.2959
		$\langle r^{-1} \rangle$	1.2261	1.2341	1.2179	1.2264
		$\langle r^{-2} \rangle$	3.3633	3.3743	3.4337	3.4973

The static dipole polarizability α, which describes the variation of the dipole moment with respect to an applied external field, was evaluated for the noble gas atoms using fully uncontracted basis sets for both WTBS and wtMCP. Table 2.3 shows a comparison of α between all-electron and wtMCP calculations. The wtMCP results differ by less than 1% from their all electron counterparts.

It is seen that the new wtMCPs show excellent agreement with the reference values. In order to establish the ability of the wtMCPs to reproduce the same quality of molecular results as seen in the atomic calculations, the wtMCPs must be tested in molecular environment. This subject is discussed in the next chapter.

Table 2.3: Static dipole polarizability (in a_0^3) for the noble-gas atoms.

Atom	Method			
	AE-NR	NR-wtMCP	AE-RESC	SR-wtMCP
Ne	0.665	0.662		
Ar	2.473	2.463		
Kr	13.797	13.750	13.801	13.764
Xe	18.602	18.634	18.600	18.583
Rn	22.779	22.731	22.439	22.369

Chapter 3

The Applications of the wtMCPs in Molecular Calculations

In the MCP formalism, a molecule can be viewed as an assembly of M non-overlapping atomic cores, with each atomic center contributing $N_{\alpha,v}$ valence electrons, where the MCP molecular hamiltonian is given by[40]

$$\hat{H}(1,2,\ldots,N_v) = \sum_{i=1}^{N_v} \hat{h}(i) + \sum_{i>j}^{N_v} \frac{1}{r_{ij}} + \sum_{\alpha>\beta}^{M} \frac{(Z_\alpha - N_{\alpha,c})(Z_\beta - N_{\beta,c})}{R_{\alpha\beta}} \quad (3.1)$$

with

$$\hat{h}(i) = -\frac{1}{2}\nabla_i^2 + \sum_{\alpha=1}^{M} \left[\hat{V}_i^{\alpha} + \hat{P}_i^{\alpha}\right] \quad (3.2)$$

and

$$N_v = \sum_{\alpha=1}^{M} N_{\alpha,v}. \quad (3.3)$$

The terms in square brackets of Eq. (3.2) are the analogues of the corresponding terms given in Eq. (1.55).

The wtMCP uses a large valence basis set designed for the MCP method. It has been seen from the previous chapter that the wtMCPs can excellently reproduce atomic properties. Prior to using the wtMCPs for predicting molecular properties of real systems, the ability of the wtMCP to reproduce the results of the all-electron molecular calculations must be established. With this in mind, testing and calibration of the new wtMCP proceeded in two steps. First, the wtMCP were tested against all-electron calculations with the same basis set that were used in the preparation of the wtMCP parameters.[1] Second, the wtMCPs were tested for real systems by comparing the calculated results against known experimental values.

[1]The results from the first step of testing and calibration have been recently published by Mane and Klobukowski[41].

3.1 Comparison of All-electron and wtMCP Results

3.1.1 Computational Method

Molecular calculations were performed at the RHF level for homonuclear diatomic molecules of several *p*-block elements; linear trihalogen ions A_3^- (A = F, Cl, Br, and I); several families of fluorinated halogen AF_3 (C_{2v}), AF_5 (C_{4v}), and AF_7 (D_{5h}), where A = F, Cl, Br, and I); and fluorides of noble gases: ArF_2, KrF_2, XeF_2, XeF_4, and XeF_6. The NR-wtMCP were compared with non-relativistic all-electron(AE) HF results. For the diatomic and triatomic ions containing halogen atoms, all-electron RESC were obtained for comparison with SR-wtMCP. For all-electron calculations, the GAMESS-US[64, 65] program was used. For the MCP calculations, the locally modified GAMESS-US and CADPAC[63] programs were used. The CADPAC program allows for the evaluation of analytical gradients as well as analytical and numerical hessians. The modified GAMESS-US program, into which the MCP code was integrated, allows at present only for evaluation of energy, *i.e.*, analytical gradients and hessians are not yet available. However, even with this limitation, equilibrium geometries can still be obtained by using the modified Powell method of searches along conjugate directions. The modified GAMESS-US program was used for the diatomic molecules, while the CADPAC[63] program was used for the triatomic ions, fluorinated halogens and fluorides of noble gases.

For the diatomic molecules, uncontracted basis functions were used. The structures of the MCP basis functions used for all other molecules are shown in Table 3.1, where the number of contracted functions in each symmetry species is followed by detailed specification of the contraction pattern. The WTBS[57, 99], contracted using the general scheme of Raffenetti[56], were used in the all-electron calculations. No polarization functions were used in any of the calculations. This was done in order to assess the reproducibility of the all-electron molecular results using parameters derived solely in atomic calculations. Due to limitations of the CADPAC molecular integral code, the $d-$type basis function with the largest exponent was uncontracted in the wtMCP calculations for molecules containing I and Xe.

Table 3.1: Contraction patterns of the AE and wtMCP basis sets (the notation 6s (8,1,1,1,1,1) denotes 6*s*−type basis functions, the first of which is an 8-term contracted function and the remaining five are uncontracted).

Atom	**Basis Set**	
	AE	wtMCP
F	7s (20,20,1,1,1,1,1)	6s (8,1,1,1,1,1)
	6p (13,1,1,1,1,1)	6p (8,1,1,1,1,1)
Cl	8s (23,23,23,1,1,1,1,1)	6s (11,1,1,1,1,1)
	7p (16,16,1,1,1,1,1)	6p (11,1,1,1,1,1)
Br	9s (26,26,26,26,1,1,1,1,1)	7s (12,3,1,1,1,1,1)
	8p (20,20,20,1,1,1,1,1)	7p (12,3,1,1,1,1,1)
	1d (14)	1d (14)
I	9s (28,28,28,28,28,1,1,1,1)	6s (13,5,1,1,1,1)
	8p (23,23,23,23,1,1,1,1)	6p (13,5,1,1,1,1)
	2d (17,17)	2d (1,16)
Ar	8s (23,23,23,1,1,1,1,1)	6s (11,1,1,1,1,1)
	7p (16 16,1,1,1,1,1)	6p (11,1,1,1,1,1)
Kr	9s (26,26,26,26,1,1,1,1,1)	7s (12,3,1,1,1,1,1)
	8p (20,20,20,1,1,1,1,1)	7p (12,3,1,1,1,1,1)
	1d (14)	1d (14)
Xe	9s (28,28,28,28,28,1,1,1,1)	6s (13,5,1,1,1,1)
	8p (23,23,23,23,1,1,1,1)	6p (13,5,1,1,1,1)
	2d (17,17)	2d (1,16)

3.1.2 Results and Discussion

Diatomic Molecules

The primitive Gaussian type functions given in Table 2.1 were fully uncontracted and used as basis functions for wtMCP calculations. The obtained results were compared with the uncontracted all-electron WTBS results. Equilibrium geometries r_e were obtained via the modified Powell method. Harmonic vibrational frequencies $\overline{\omega}_e$ were obtained by fitting the total energy curve at several points bracketing the equilibrium. Tables 3.2 and 3.3 show the comparison of optimized geometries and vibrational frequencies, respectively, obtained in AE and wtMCP calculations.

Table 3.2: Optimized geometries (in Å) of homonuclear diatomic molecules.

Molecule	Method			
	AE-NR	NR-wtMCP	AE-RESC	SR-wtMCP
C_2	1.2567	1.2561		
Si_2	2.1334	2.1326		
Ge_2	2.1849	2.1800	2.1758	2.1692
Sn_2	2.5757	2.5681	2.5483	2.5419
Pb_2	2.7507	2.7432	2.6559	2.6497
N_2	1.0835	1.0824		
P_2	1.9376	1.9351		
As_2	2.0649	2.0572	2.0573	2.0493
Sb_2	2.4690	2.4584	2.4456	2.4353
Bi_2	2.6601	2.6510	2.5759	2.5679
O_2	1.1945	1.1942		
S_2	2.0041	2.0028		
Se_2	2.1445	2.1387	2.1399	2.1333
Te_2	2.5564	2.5449	2.5405	2.5305
Po_2	2.7626	2.7541	2.6954	2.6901
F_2	1.3786	1.3787		
Cl_2	2.1315	2.1294		
Br_2	2.2912	2.2873	2.2878	2.2825
I_2	2.7045	2.6940	2.6915	2.6803
At_2	2.9216	2.9143	2.8616	2.8547

Table 3.3: Vibrational frequencies $\overline{\omega}_e$ (in cm^{-1}) for diatomic molecules.

Molecule	Method			
	AE-NR	NR-wtMCP	AE-RESC	SR-wtMCP
C_2	1812.7	1808.7		
Si_2	552.6	551.0		
Ge_2	345.7	344.8	344.0	343.6
Sn_2	227.3	226.6	225.7	225.1
N_2	2563.4	2560.5		
P_2	797.1	795.7		
As_2	507.9	508.1	506.4	506.6
Sb_2	326.6	326.5	325.8	325.8
Bi_2	226.9	227.3	229.6	231.0
O_2	1829.0	1825.2		
S_2	699.5	699.6		
Se_2	436.9	437.1	435.4	435.3
Te_2	283.0	283.87	281.3	281.6
Po_2	203.3	203.6	204.5	204.5
F_2	1189.2	1188.5		
Cl_2	550.1	550.2		
Br_2	349.5	349.3	348.7	348.6
I_2	231.9	232.5	231.3	231.5
At_2	165.5	165.9	166.2	166.8

The mean error in the equilibrium internuclear distance is small – 0.0052 Å at the non-relativistic level and 0.0057 Å at the scalar-relativistic level. For the harmonic vibrational frequencies, the mean errors are 1.0 cm^{-1} and 0.7 cm^{-1} for the non-relativistic and scalar-relativistic levels, respectively.

The mean error was determined by the following general formula:

$$\sigma(X) = \sum_{i=1}^{N} \frac{\left|X_i^{calc} - X_i^{ref}\right|}{N} \tag{3.4}$$

where X is the property of interest (in this case, r_e and $\overline{\omega}_e$) and N is the number of molecules studied.

Triatomic Halide Ions

Table 3.4 shows the results for triatomic halide anions. The bond length errors are similar to the ones found in diatomic halides (Tables 3.2 and 3.3), while the vibrational frequencies agree less well, with the maximum error reaching 4% for the Π_u mode of F_3^-. The F_3^- ion demonstrates how faithfully the wtMCP method reproduces the results of the AE calculations: at the RHF level the linear $D_{\infty h}$ structure is a saddle point with the imaginary frequency corresponding to the asymmetric stretch Σ_u^+[115]. It may be noted here that both the old MCPs[60] and the popular CEPs[69] fail to reproduce the character of the accurate RHF potential energy surface. The relativistic shortening of the bonds is more pronounced than that seen in the diatomics, reaching 0.041 Å for I_3^-. The all-electron RESC values of the bond lengths were again obtained via interpolation of total energies calculated at points bracketing the equilibrium internuclear distance and assuming linear structure of the ion. The differences between the RESC and SR-wtMCP bond lengths are of the same magnitude as those found at the non-relativistic level, with the largest found again for I_3^-. The relativistic bond contraction at the wtMCP level is similar to that found at the all-electron level with the exception of Cl_3^-, where the wtMCP contraction is too large.

Table 3.4: Results for A_3^- ions (A = F, Cl, Br, I; bond lengths r_e in Å, vibrational frequencies $\overline{\omega}_e$ in cm^{-1} defined by the symmetry of the normal modes).

Molecule	Property	Method			
		AE-NR	NR-wtMCP	AE-RESC	SR-wtMCP
F_3^-	r_e	1.6621	1.6617	1.6617	1.6609
	Σ_u^+	405.5i	330.3i	404.9	342.5i
	Π_u	334.5	348.4	334.5	353.6
	Σ_g^+	551.7	554.6	552.2	553.5
Cl_3^-	r_e	2.4161	2.4136	2.4131	2.4116
	Π_u	153.7	160.5	153.7	160.4
	Σ_g^+	215.8	220.7	218.0	223.2
	Σ_u^+	266.9	268.1	267.2	268.3
Br_3^-	r_e	2.6775	2.6704	2.6607	2.6573
	Π_u	88.4	93.8	87.7	93.7
	Σ_g^+	158.2	158.6	162.9	161.7
	Σ_u^+	160.7	160.8	167.6	163.0

continued on next page

Table 3.4: *continued*

Molecule	Property	Method			
		AE-NR	NR-wtMCP	AE-RESC	SR-wtMCP
I_3^-	r_e	3.0960	3.0918	3.0594	3.0511
	Π_u	56.8	57.3		56.9
	Σ_u^+	108.2	108.0		110.6
	Σ_g^+	117.4	120.3		130.8

Fluorinated Halogens

The planar T-shape structure with symmetry C_{2v} was assumed for ClF_3, BrF_3, and IF_3. The results in Table 3.5 show that the wtMCP equilibrium structures agree very well with the AE ones, the largest error seen for the axial bond in IF_3 that is too short by 0.003 Å. The wtMCP values of the dipole moment closely follow the all-electron values, with the largest error less than 1%. The error in the vibrational frequencies is the largest for the dihedral bend B_2 (about 15 cm^{-1} too large for ClF_3 and BrF_3). The relativistic bond contraction is virtually absent; in fact, the equatorial bonds are longer in the scalar-relativistic calculations. Similar lengthening of bonds was found in the studies of XeF_6 and related systems[116].

Table 3.5: Results for AF_3 molecules (A = Cl, Br, I; bond lengths r_e in Å, the angle $\phi = F_{ax}$-A-F_{eq} in degrees, dipole moments μ in Debye, vibrational frequencies $\overline{\omega}_e$ in cm^{-1} defined by the symmetry of the normal modes).

Molecule	Property	Method		
		AE-NR	NR-wtMCP	SR-wtMCP
ClF_3	r_e (ax)	1.6787	1.6793	1.6789
	r_e (eq)	1.8043	1.8050	1.8050
	ϕ	85.15	85.15	85.26
	μ	1.206	1.196	1.188

continued on next page

Table 3.5: *continued*

Molecule	Property	Method		
		AE-NR	NR-wtMCP	SR-wtMCP
	B_2	290.9	305.4	302.3
	A_1	303.9	311.0	311.1
	B_1	395.9	403.5	401.6
	A_1	539.4	545.6	545.3
	B_1	650.6	652.8	652.7
	A_1	798.1	801.2	801.2
BrF_3	r_e (ax)	1.7671	1.7646	1.7640
	r_e (eq)	1.8723	1.8696	1.8714
	ϕ	83.88	84.00	84.60
	μ	2.289	2.298	2.278
	B_2	242.9	257.4	251.3
	A_1	256.6	261.0	257.3
	B_1	356.9	362.5	353.4
	A_1	550.9	556.0	558.0
	B_1	575.8	578.1	578.6
	A_1	707.0	710.2	713.5
IF_3	r_e (ax)	1.9081	1.9048	1.9042
	r_e (eq)	1.9859	1.9843	1.9896
	ϕ	81.06	81.25	83.15
	μ	3.668	3.681	3.760
	B_2	205.3	205.6	198.3
	A_1	224.2	222.4	207.1
	B_1	319.3	318.9	295.6
	A_1	556.0	556.0	557.2
	B_1	569.8	567.9	562.9
	A_1	674.8	673.5	670.3

In the calculations for the AF_5 molecules the C_{4v} symmetry of the nuclear framework was assumed. The results in Table 3.6 show that the agreement between the geometries of the AF_5 molecules from the AE and wtMCP calculations is excellent, the largest error being seen for the axial bond in IF_5 (too short by 0.004 Å). The wtMCP values of the dipole moment are again within 1% of the all-electron values. Vibrational frequencies are less well reproduced, with the errors reaching 34 cm^{-1} (the B_2 mode in ClF_5). As in the case of AF_3 molecules, the equatorial bonds are longer at the scalar-relativistic level.

Table 3.6: Results for AF_5 molecules (A = Cl, Br, I; bond lengths r_e in Å, the angle $\phi = F_{ax}$-A-F_{eq} in degrees, dipole moments μ in Debye, vibrational frequencies $\overline{\omega}_e$ in cm^{-1} defined by the symmetry of the normal modes).

Molecule	Property	Method		
		AE	NR-wtMCP	SR-wtMCP
ClF_5	r_e (ax)	1.7287	1.7315	1.7286
	r_e (eq)	1.7659	1.7668	1.7676
	ϕ	84.03	84.01	84.09
	μ	1.507	1.494	1.461
	E	234.8	254.4	253.9
	B_1	239.2	250.0	248.5
	B_2	266.9	295.6	294.9
	E	379.2	401.7	401.4
	A_1	448.7	466.0	465.8
	B_1	471.7	468.8	469.6
	A_1	514.7	521.9	520.6
	A_1	664.1	668.5	668.4
	E	749.1	754.1	753.1
BrF_5	r_e (ax)	1.7600	1.7562	1.7534
	r_e (eq)	1.8206	1.8178	1.8224
	ϕ	83.05	83.15	83.57
	μ	2.622	2.627	2.545
	E	210.2	225.7	222.8
	B_1	216.6	233.7	226.9
	B_2	229.0	241.0	242.4
	E	349.8	364.0	358.5
	A_1	384.6	397.5	380.2
	B_1	546.8	549.4	551.5
	A_1	549.6	552.3	558.7
	E	641.1	642.3	642.6
	A_1	657.1	661.9	664.7

continued on next page

Table 3.6: *continued*

Molecule	Property	Method		
		AE	NR-wtMCP	SR-wtMCP
IF_5	r_e (ax)	1.8694	1.8653	1.8620
	r_e (eq)	1.9234	1.9213	1.9307
	ϕ	80.73	80.89	81.99
	μ	4.287	4.287	4.342
	B_1	147.7	151.4	165.2
	E	172.7	174.3	169.2
	B_2	206.7	206.6	188.1
	E	321.0	321.3	308.7
	A_1	343.2	339.8	304.3
	B_1	585.6	587.6	581.7
	A_1	586.6	589.7	593.3
	E	640.9	639.4	627.3
	A_1	689.2	689.7	687.7

Very good results are obtained also for the AF_7 molecules (Table 3.7) - with the largest error of 0.003 Å for the axial bond in BrF_7 and 16 cm^{-1} for the first A_1' mode. The SR-wtMCP calculations show bond lengthening for all systems. As expected, the imaginary frequency $\overline{\omega}_e(E_2'')$ indicates that the assumed D_{5h} symmetry does not correspond to the minimum on the potential energy surface.

Table 3.7: Results for AF_7 molecules (A = Cl, Br, I; bond lengths r_e in Å, vibrational frequencies $\overline{\omega}_e$ in cm^{-1} defined by the symmetry of the normal modes).

Molecule	Property	Method		
		AE-NR	NR-wtMCP	SR-wtMCP
ClF_7	r_e (ax)	1.7066	1.7083	1.7090
	r_e (eq)	1.8493	1.8509	1.8517
	E_2''	61.8i	59.5i	57.8i
	E_1'	229.3	228.4	228.0
	E_1''	239.2	242.3	242.3
	E_2'	332.7	334.7	332.3
	A_2''	338.3	337.8	335.6
	E_1'	472.3	470.6	468.3
	A_1'	493.2	494.4	492.8
	E_2'	552.3	550.3	548.0

continued on next page

Table 3.7: *continued*

Molecule	Property	Method		
		AE	NR-wtMCP	SR-wtMCP
	A_1'	568.2	572.1	569.0
	E_1'	595.2	596.0	591.8
	A_2''	844.5	845.3	842.4
BrF_7	r_e (ax)	1.7546	1.7516	1.7594
	r_e (eq)	1.8537	1.8529	1.8592
	E_2''	118.6i	119.7i	113.6i
	E_1'	171.6	179.6	187.8
	E_1''	210.0	214.1	214.7
	A_2''	309.0	307.7	305.8
	E_2'	417.5	416.9	416.8
	E_1'	447.6	453.3	447.9
	A_1'	537.1	553.5	546.3
	E_2'	579.2	578.5	568.1
	E_1'	579.3	579.2	568.8
	A_1'	609.4	610.6	606.9
	A_2''	727.0	726.6	717.0
IF_7	r_e (ax)	1.8547	1.8520	1.8636
	r_e (eq)	1.9091	1.9077	1.9201
	E_2''	158.0i	156.0i	144.2i
	E_1'	29.1	31.2	85.8
	E_1''	138.8	138.4	143.7
	A_2''	246.6	251.1	248.0
	E_2'	398.2	400.5	390.4
	E_1'	492.4	494.1	481.1
	E_2'	554.4	556.0	541.9
	A_1'	623.0	628.5	602.2
	E_1'	664.8	663.7	633.6
	A_1'	670.1	671.8	653.1
	A_2''	748.1	747.0	716.9

Noble-Gas Fluorides

In order to test the performance of the wtMCPs prepared for the noble gas atoms, calculations were carried out for several noble-gas fluorides. The triatomic systems were studied in $D_{\infty h}$ symmetry, XeF_4 – in D_{4h}, and XeF_6 – in O_h symmetry. Again, excellent agreement between the AE and NR-wtMCP results may be seen for these molecules (Table 3.8). The bond lengths differ by a maximum of 0.0025 Å and vibrational frequencies by less than 10 cm^{-1}. As found in other calculations[116, 117], the octahedral structure of XeF_6 is not a minimum on the potential energy surface with the first T_{1u} mode leading to a structure with lower symmetry and lower total energy.

Table 3.8: Results for noble-gas fluorides (bond lengths r_e in Å, vibrational frequencies $\overline{\omega}_e$ in cm^{-1} defined by the symmetry of the normal modes).

Molecule	**Property**	**Method**		
		AE-NR	NR-wtMCP	SR-wtMCP
ArF_2	r_e	1.8602	1.8600	-
	Π_u	263.1	272.7	-
	Σ_g^+	504.1	506.0	-
	Σ_u^+	626.9	629.1	-
KrF_2	r_e	1.9280	1.9267	1.9223
	Π_u	237.7	241.7	240.7
	Σ_g^+	529.6	534.0	537.3
	Σ_u^+	558.8	562.1	566.4
XeF_2	r_e	2.0425	2.0414	2.0344
	Π_u	219.4	219.4	214.1
	Σ_u^+	515.8	517.1	532.5
	Σ_g^+	522.9	524.6	536.7
XeF_4	r_e	2.0115	2.0104	1.9980
	E_u	89.6	94.8	125.7
	B_{2g}	166.8	166.9	163.5
	B_{1g}	199.7	203.3	213.0
	A_{2u}	276.7	276.3	266.7
	B_{2g}	518.3	519.9	539.0
	A_{1g}	535.4	540.0	556.9
	E_u	543.9	545.1	571.3

continued on next page

Table 3.8: *continued*

Molecule	Property	Method		
		AE-NR	NR-wtMCP	SR-wtMCP
XeF_6	r_e	2.0037	2.0012	1.9798
	T_{1u}	246.3i	238.2i	155.7i
	T_{2u}	65.1	65.5	82.9
	T_{2g}	67.0	68.2	105.0
	E_g	492.4	497.5	525.8
	T_{1u}	534.5	536.9	583.7
	A_{1g}	547.2	550.5	583.9

The present results clearly show that the model core potential method developed in atomic calculations carries the excellent agreement from the atomic to molecular environment without the need for any adjustment. The method is fully able to reproduce geometries and vibrational frequencies of the reference all-electron calculations despite the use of the local potential, provided that the valence basis sets are sufficiently large. The comparison was done at the RHF level; as discussed in Chapter 1, electron correlation may be required for comparison with the experimental data. The question whether the new wtMCPs may be safely used in the post-Hartree-Fock calculations is discussed in the next section.

3.2 Comparison of Experimental and wtMCP Results

In the previous section, promising results were obtained using the wtMCPs at the RHF level. If wtMCPs are to be used in predicting molecular properties of real systems, as an alternative to the expensive all-electron *ab initio* calculations, it is necessary to know how well the wtMCPs can reproduce the experimental results.

In this section, results of preliminary tests are reported. However, the intention is not to fully discuss every result obtained but to show a general idea how good and effective the wtMCPs are in providing close approximation to the experimental results.

3.2.1 Computational Method

Molecular calculations that include electron correlation were done at the MP2 and DFT (using the B3P91 functional) levels for several molecular systems to determine how well the new wtMCP potentials reproduce experimental values. The molecular systems studied were group 13 halides (BF, AlCl, GaBr, InI), group 14 sulfides AS (A = C, Si, Ge, Sn) and interhalogen diatomic compounds; several families of trihydrogen pnictides AH_3 (A = N, P, As, Sb) and dihydrogen chalcogenides AH_2 (A = O, S, Se, Te). RHF calculations were also performed to serve as reference in the absence of electron correlation. The locally modified version of CADPAC[63] computer package was used for all calculations. Analytical gradients were used in the geometry optimization. The harmonic vibrational frequencies were evaluated using numerically determined hessians.

The structure of the wtMCP basis functions used for all calculations are shown in Table 3.9, in which the number of contracted functions in each symmetry is followed by detailed specification of the contraction pattern. A set of double $d-$ type polarization functions taken from Sadlej medium-sized polarized basis sets[118, 119], were used for the members of the first two rows of the periodic table. For compounds containing hydrogen, Sadlej polarized basis set was used for the lightest atom[118].

Table 3.9: wtMCP basis set contractions for atoms used in correlation studies (the notation 4s (8,2,1,2) denotes $4s-$type basis functions, the first of which is an 8-term contracted function, followed by a 2-term contracted function, an uncontracted function and the last being a 2-term contracted function).

Atom	**Basis set**
B - F	4s (8,2,1,2) 4p (8,2,1,2)
Al - Cl	5s (8,3,2,1,2) 5p (8,3,2,1,2)
Ga - Br	5s (12,3,2,1,2) 5p (12,3,2,1,2) 3d (10,2,2)
In - I	5s (13,5,2,1,2) 5p (13,5,2,1,2) 3d (11,4,2)
H	3s (4,1,1) 2p (2,2)

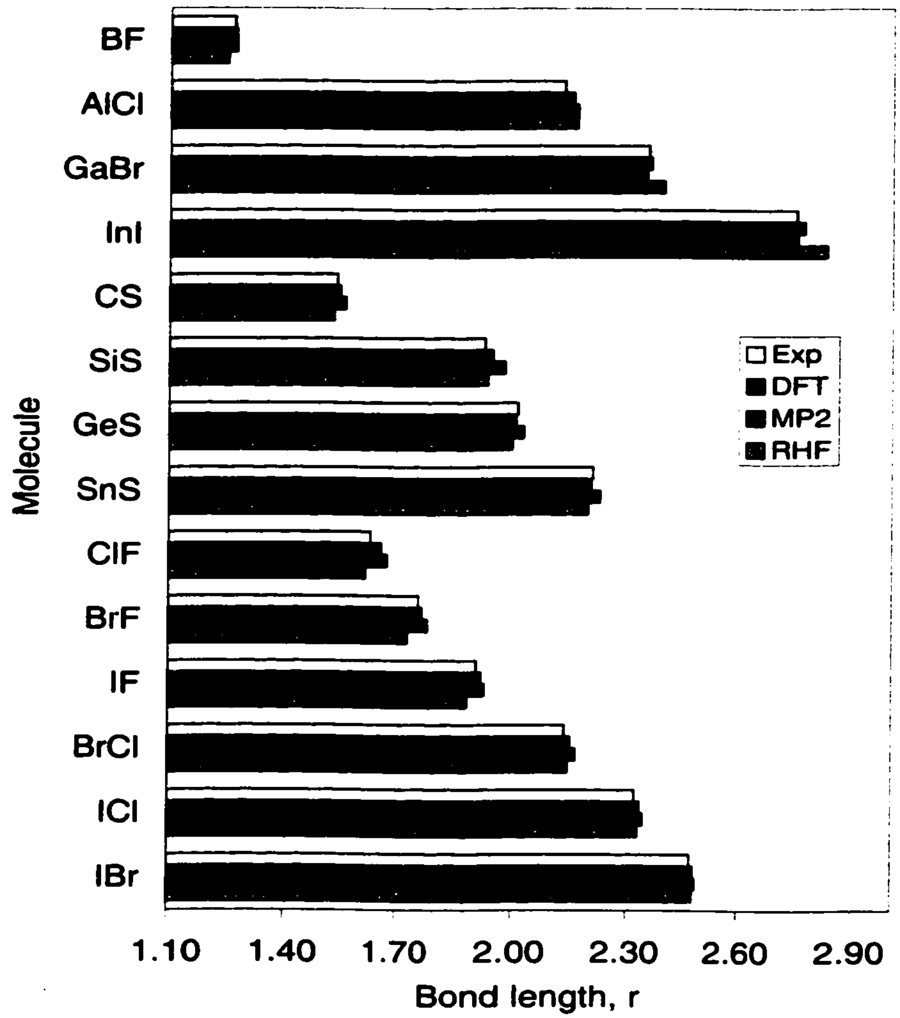

Figure 3.1: Comparison of calculated and experimental bond lengths (in Å) for diatomic molecules.

3.2.2 Results and Discussion

The complete listing of results comparing both NR-wtMCPs and SR-wtMCPs to experimental data can be found in Tables A.1 - A.5 in the Appendix A. The experimental data used were taken from the compilation of Huber and Herzberg[120].

In order to give some idea on how good the wtMCPs are, NR-wtMCP(for light atoms) and SR-wtMCP (for heavy atoms) results for selected diatomic and polyatomic hydrogen molecules were presented. Figures 3.1 and 3.2 present graphical comparisons of the performance of wtMCP results, both at HF and post-HF levels, and the experimentally determined bond lengths and harmonic vibrational frequencies. Excellent agreement was found between the experimental and the wtMCP results for the diatomic molecules.

At the RHF level alone, the calculated bond lengths are often close to the

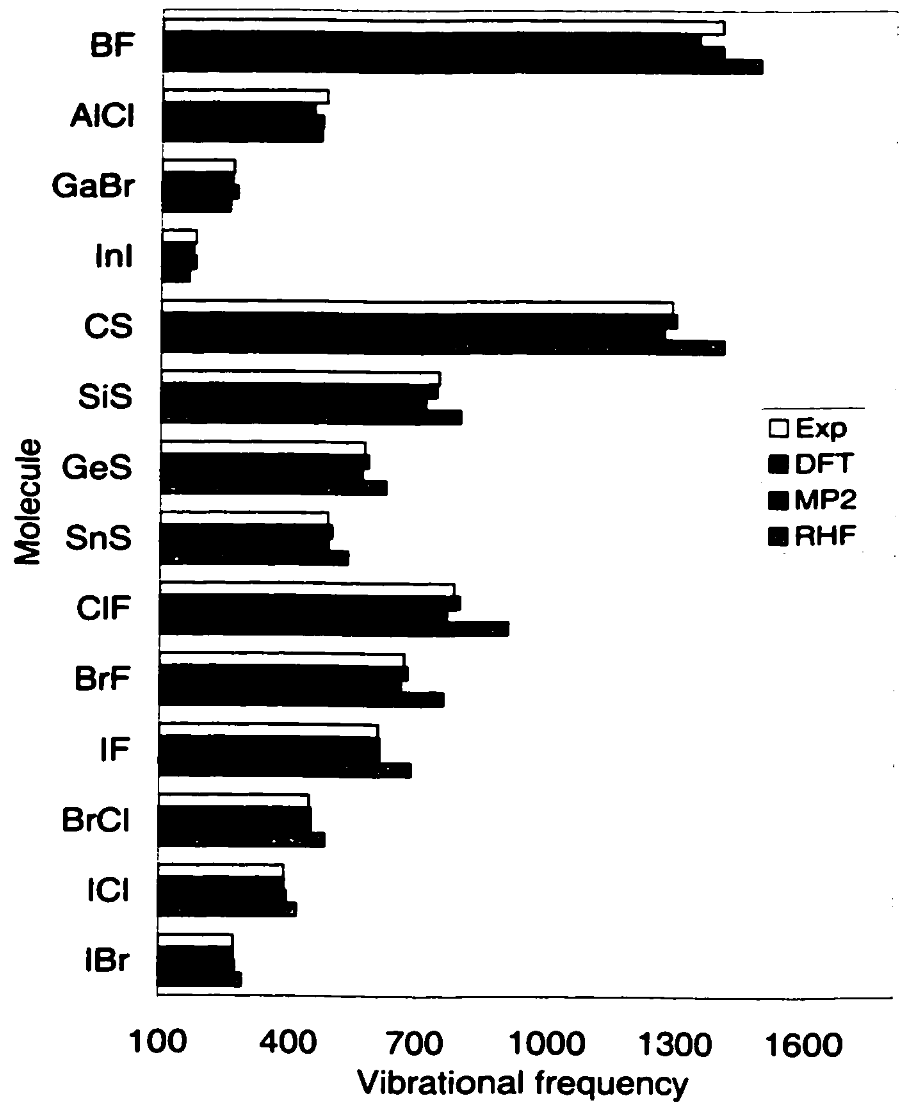

Figure 3.2: Comparison of calculated and experimental vibrational frequencies (in cm^{-1}) for diatomic molecules.

experimental values. However, the RHF vibrational frequencies are usually too large (with the exception of AlCl, GaBr and InI), reflecting the fact that the RHF wavefunction usually does not dissociate to correct atomic states and thus leads to potential energy curves that are too steep near the minimum. A noticeable improvement is seen when correlated methods are used in which DFT results appear to give better agreement with experiment than MP2 results.

Similar calculations were performed for trihydrogen pnictides and dihydrogen chalcogenides (TablesA.4 and A.5) to determine how well the wtMCPs compare with experimental structural data for polyatomic systems. Figures 3.3 and 3.4 compare the calculated wtMCP and experimentally determined bond

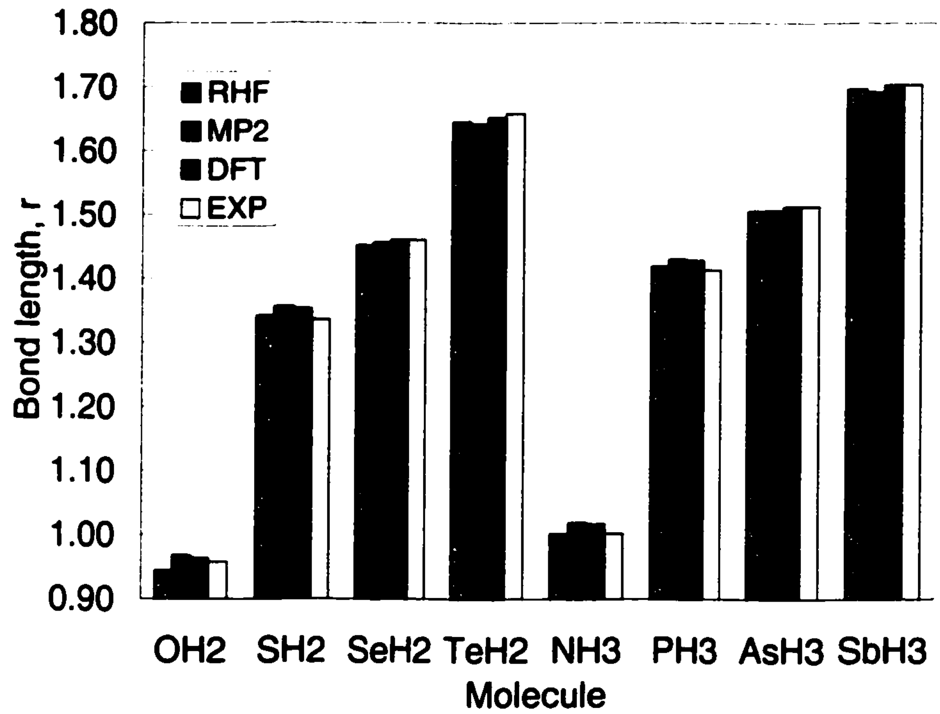

Figure 3.3: Comparison of calculated and experimental bond lengths (in Å) for AH_2 and AH_3 (A = O, S, Se, Te, N, P, As, Sb) molecules.

lengths and bond angles, respectively. Experimental bond lengths are already well reproduced even at the RHF level. However, the RHF bond angles overshoot experimental values indicating that a pure HF treatment alone is insufficient to describe the correct geometry and that correlation is necessary. At the MP2 and DFT levels, the calculated structural parameters are very close to the experimental values. Again, DFT performs better than MP2.

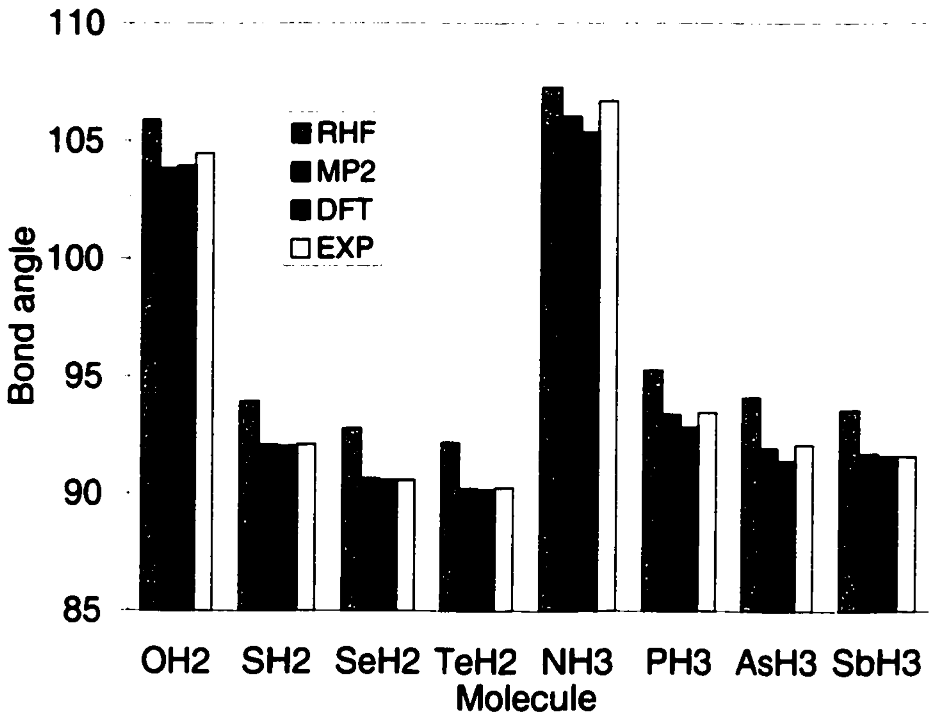

Figure 3.4: Comparison of calculated and experimental angles (in degrees) for AH_2 and AH_3 (A = O, S, Se, Te, N, P, As, Sb) molecules.

Chapter 4

Conclusions and Future Prospects

A new family of MCP pseudopotentials, based on the well-tempered basis set expansion, has been developed for the main-group elements from Li to Rn of the periodic table. They have been tested in atomic and molecular calculations at both the Hartree-Fock and post-Hartree Fock levels. The present development of the well-tempered model core potentials shows promising results in reproducing the computationally expensive all-electron results. The wtMCPs are capable of reproducing geometries and vibrational frequencies accurately even though only local potentials are being used to represent the valence-core interactions.

The wtMCPs were developed via fitting to a fully analytical all-electron HF or RESC reference functions. The new wtMCPs are designed to have a very flexible valence basis set in which the levels of contraction can be tailored to the requirements of the computation for specific problems or applications. No matter how they are contracted, calculations are only affected by the relatively inexpensive integral evaluations.

The wtMCP expansions of the valence orbitals are large. However, wtMCP basis sets may be conveniently folded into a contracted L-shell basis set made possible by the shared exponents available in the well-tempered basis set. Significant computational savings can be attained by reducing the integral evaluation time, provided that the integral code in the computer program uses L-shell structure. The reduction in computing time with respect to the all-electron calculations is important if fast but accurate results are necessary and if computing resources are limited. In fact, the reduction in computing time achieved in going from all-electron WTBS to using wtMCP is about 50-100 times, while retaining the same accuracy of results.

The new wtMCP basis sets are slower compared to their ECP competitors. However, this obstacle to the use of the wtMCPs in very accurate pseudopotential calculations will be surely removed since computers are becoming both more powerful and affordable.

The preliminary results presented in this thesis are encouraging. There are several issues that must still be resolved in future developments. In particular, the new wtMCPs must be tested for their effectiveness in reproducing molecular properties other than the structural parameters and harmonic vibrational frequencies studied in the present work.

Another interesting future work is to study the performance of the MCP model itself using the wtMCP basis sets in evaluating valence-electron correlation energies in atoms and molecules. In the MCP model, the core orbitals are shifted into the virtual orbital space by the projection operators which might result in overestimation of the electron correlation energies.

An interesting feature of the new wtMCPs is the retention of the full nodal structure of the valence reference orbitals. The accurate nodal structure allows for an accurate description of the region close to the nucleus. With the development of the SR-wtMCP based on the RESC method, these new wtMCP pseudopotentials can be ideal tools for spin-orbit studies without the need for scaling[49].

Bibliography

[1] A. Szabo and N. S. Ostlund. *Modern Quantum Chemistry*. Dover Publications, Inc., Mineola, New York, 1996.

[2] I. N. Levine. *Quantum Chemistry*. Prentice Hall, Upper Saddle River, New Jersey, 5th edition, 2000.

[3] F. Jensen. *Introduction to Computational Chemistry*. John Wiley & Sons, Chichester, West Sussex, England, 1999.

[4] D. A. McQuarrie. *Quantum Chemistry*. University Science Books, Sausalito, California, 1983.

[5] C. C. J. Roothaan. *Rev. Mod. Phys.*, 23:69, 1951.

[6] G. G. Hall. *Proc. R. Soc. A*, 205:541, 1951.

[7] K. Raghavachari. Electron correlation techniques in quantum chemistry. *Annu. Rev. Phys. Chem.*, 42:615–642, 1991.

[8] S. Saebo and P. Pulay. Local treatment of electron correlation. *Annu. Rev. Phys. Chem.*, 44:213–236, 1993.

[9] K. Raghavachari. Electron correlation effects in molecules. *J. Phys. Chem.*, 100:12960–12973, 1996.

[10] R. J. Bartlett. Coupled-cluster approach to molecular structure and spectra: A step toward predictive quantum chemistry. *J. Phys. Chem.*, 93:1697–1708, 1989.

[11] C. Møller and M. S. Plesset. *Phys. Rev.*, 46:618, 1934.

[12] R. Krishnan and J. A. Pople. Approximate fourth-order perturbation theory of the electron correlation energy. *Int. J. Quantum Chem.*, 14:91–100, 1978.

[13] P. Hohenberg and W. Kohn. *Phys. Rev. B*, 136:864, 1964.

[14] R. G. Parr and W. Yang. *Density-Functional Theory of Atoms and Molecules*. Oxford University Press, Inc., New York, 1989.

[15] W. Kohn and L. J. Sham. *Phys. Rev. A*, 140:1133, 1965.

[16] R. Stowasser and R. Hoffmann. What do the Kohn-Sham orbitals and eigenvalues mean? *J. Am. Chem. Soc.*, 121:3414–3420, 1999.

[17] P. Bouř. Comparison of Hartree-Fock and Kohn-Sham determinants as wavefunction. *J. Comput. Chem.*, 21:8–16, 2000.

[18] D. M. Ceperley and B. J. Alder. Ground-state of the electron-gas by a stochastic method. *Phys. Rev. Lett.*, 45:566–569, 1980.

[19] S. H. Vosko, L. Wilk, and M. Nusair. Accurate spin-dependent electron liquid correlation energies for local spin-density calculations – a critical analysis. *Can. J. Phys.*, 58:1200–1211, 1980.

[20] A. D. Becke. Density-functional exchange-energy approximation with correct asymptotic behavior. *Phys. Rev. A*, 38:3098, 1988.

[21] A. D. Becke. Density-functional thermochemistry. IV. A new dynamical correlation functional and implications for exact-exchange mixing. *J. Chem. Phys.*, 104:1040, 1996.

[22] A. D. Becke. Density-functional thermochemistry. V. Systematic optimization of exchange-correlation functionals. *J. Chem. Phys.*, 107:8554, 1997.

[23] J. P. Perdew. Density-functional approximation for the correlation energy of the inhomogeneous electron gas. *Phys. Rev. B*, 33:8822, 1986.

[24] J. P. Perdew and Y. Wang. Accurate and simple density functional for the electronic exchange energy: Generalized gradient approximation. *Phys. Rev. B*, 33:8800, 1986.

[25] C. Lee, W. Yang, and R. G. Parr. Development of the Colle-Salvetti correlation-energy formula into a functional of the electron density. *Phys. Rev. B*, 37:785, 1988.

[26] A. D. Becke. Density-functional thermochemistry: III. The role of exact exchange. *J. Chem. Phys.*, 98:5648, 1993.

[27] H. Hellmann. *J. Chem. Phys.*, 3:61, 1935.

[28] L. Szasz. *Pseudopotential Theory of Atoms and Molecules.* John Wiley & Sons, New York, 1985.

[29] V. Bonifacic and S. Huzinaga. Atomic and molecular calculations with the model potential method. I. *J. Chem. Phys.*, 60:2779, 1974.

[30] V. Bonifacic and S. Huzinaga. Atomic and molecular calculations with the model potential method. II. *J. Chem. Phys.*, 62:1507, 1975.

[31] V. Bonifacic and S. Huzinaga. Atomic and molecular calculations with the model potential method. III. *J. Chem. Phys.*, 62:1509, 1975.

[32] V. Bonifacic and S. Huzinaga. Atomic and molecular calculations with the model potential method. IV. *J. Chem. Phys.*, 64:956, 1976.

[33] V. Bonifacic and S. Huzinaga. Atomic and molecular calculations with the model potential method. V. *J. Chem. Phys.*, 65:2322, 1976.

[34] Y. Sakai and S. Huzinaga. The use of model potentials in molecular calculations. I. *J. Chem. Phys.*, 76:2537–2551, 1982.

[35] Y. Sakai and S. Huzinaga. The use of model potentials in molecular calculations. II. *J. Chem. Phys.*, 76:2552–2557, 1982.

[36] V. Bonifacic and S. Huzinaga. Model potential calculations for HF and HCl. *Chem. Phys. Lett.*, 36:573, 1975.

[37] S. Huzinaga. Effective hamiltonian method for molecules. *J. Mol. Struc. (THEOCHEM)*, 234:51–73, 1991.

[38] S. Huzinaga. 1994 Polanyi Award Lecture: Concept of active electrons in molecules. *Can. J. Chem.*, 73:619–628, 1995.

[39] S. Huzinaga. The ab initio model potential method and the optimized orbitals for the multiconfiguration self-consistent field-configuration interaction approach. *Int. J. Quantum Chem.*, 60:83–90, 1996.

[40] M. Klobukowski, S. Huzinaga, and Y. Sakai. Model core potentials: Theory and applications. In J. Leszczynski, editor, *Computational Chemistry: Reviews of Current Trends*, volume 3. World Scientific, 1999.

[41] J. Y. Mane and M. Klobukowski. Well-tempered model core potentials for group 17 and 18. *J. Mol. Struc. (THEOCHEM)*, 547:163–170, 2001.

[42] G. Höjer and J. Chung. Some aspects of the model potential method. *Int. J. Quantum Chem.*, 14:623–634, 1978.

[43] M. Dolg. Effective core potential. In J. Grotendorst, editor, *Modern Methods and Algorithms of Quantum Chemistry*, volume 1. John von Neumann Institute for Computing, Jülich, 2000.

[44] G. Frenking, I. Antes, M. Böhme, S. Dapprich, A. W. Ehlers, V. Jonas, A. Neuhaus, M. Otto, R. Stegmann, A. Veldkamp, and S. Vyboishchikov. Pseudopotential calculatons of transition metal compounds: Scope and limitation. In K. B. Lipkowitz and D. B. Boyd, editors, *Reviews in Computational Chemistry*, volume 8. VCH Publishers, Inc. New York, 1996.

[45] T. R. Cundari, M. T. Benson, M. L. Lutz, and S. O. Sommerer. Effective core potential approaches to the chemistry of the heavier elements. In K. B. Lipkowitz and D. B. Boyd, editors, *Reviews in Computational Chemistry*, volume 8. VCH Publishers, Inc. New York, 1996.

[46] K. G. Dyall. Formal analysis of effective core potential methods. *J. Chem. Inf. Comput. Sci.*, 41:30–37, 2001.

[47] P. Schwerdtfeger, T. Fischer, M. Dolg, G. Igel-Mann, A. Nicklass, H. Stoll, and A. Haaland. The accuracy of pseudopotential approximation. I. An analysis of the spectroscopic constants for the electronic ground states of InCl and $InCl_3$ using various three valence electron pseudopotentials for indium. *J. Chem. Phys.*, 102:2050, 1995.

[48] T. Leininger, A. Nicklass, H. Stoll, M. Dolg, and P. Schwerdtfeger. The accuracy of pseudopotential approximation. II. A comparison of various core sizes for indium pseudopotentials in calculations for spectroscopic constants of InH, InF, and InCl. *J. Chem. Phys.*, 105:1052, 1996.

[49] D. Krause and M. Klobukowski. On the performance of molecular model core potential orbitals in spin-orbit and electron correlation studies. *Can. J. Chem.*, 74:1248–1252, 1996.

[50] M. Klobukowski. Atomic correlation energies from effective-core-potential and model-potential calculations. *Chem. Phys. Lett.*, 172:361, 1990.

[51] P. Pyykkö. Relativistic effects in structural chemistry. *Chem. Rev.*, 88:563, 1988.

[52] R. D. Cowan and D. C. Griffin. Approximate relativistic corrections to atomic radial wave-functions. *J. Opt. Soc. Am.*, 66:1010–1014, 1976.

[53] S. Huzinaga (ed), J. Andzelm, M. Klobukowski, E. Radzio-Andzelm, Y. Saski, and H. Tatewaki. *Gaussian Basis Sets for Molecular Calculation.* Elsevier, Amsterdam, 1984.

[54] D. Feller and E. R. Davidson. Basis set selection for molecular calculations. *Chem. Rev.*, 86:681–696, 1986.

[55] D. Feller and E. R. Davidson. Basis sets for ab initio molecular orbital calculations and intermolecular interactions. In K. B. Lipkowitz and D. B. Boyd, editors, *Reviews in Computational Chemistry*, volume 1. VCH Publishers, Inc. New York, 1990.

[56] R. C. Raffenetti. General contraction of gaussian atomic orbitals: Core, valence, polarization and diffuse basis sets; molecular integral evaluation. *J. Chem. Phys.*, 58:4452–4458, 1973.

[57] S. Huzinaga, M. Klobukowski, and H. Tatewaki. The well-tempered GTF basis-sets and their applications in the SCF calculations on N_2, CO, Na_2 and P_2. *Can. J. Chem.*, 63:1812–1828, 1985.

[58] Y. Sakai, E. Miyoshi, M. Klobukowski, and S. Huzinaga. Model potentials for molecular calculations. 1. The SD-MP set for transition-metal atoms Sc through Hg. *J. Comput. Chem.*, 8:226–255, 1987.

[59] Y. Sakai, E. Miyoshi, M. Klobukowski, and S. Huzinaga. Model potentials for molecular calculations. 2. The SPD- MP set for transition-metal atoms Sc through Hg. *J. Comput. Chem.*, 8:256–264, 1987.

[60] Y. Sakai, E. Miyoshi, M. Klobukowski, and S. Huzinaga. Model potentials for main group elements Li through Rn. *J. Chem. Phys.*, 106:8084, 1997.

[61] S. A. Decker and M. Klobukowski. Calibration and benchmarking of model core potentials: applications to systems containing main-group elements. *J. Mol. Struct. (THEOCHEM)*, 451:215–226, 1998.

[62] S. A. Decker and M. Klobukowski. Benchmarking of model core potentials: Application to the halogen complexes of Group 4 metals. *J. Chem. Inf. Comput. Sci.*, 41:1–7, 2001.

[63] R. D. Amos, I. L. Alberts, J. S. Andrews, S. M. Colwell, N. C. Handy, D. Jayatilaka, P. J. Knowles, R. Kobayashi, K. E. Laidig, G. Laming, A. M. Lee, P. E. Maslen, C. W. Murray, J. E. Rice, E. D. Simandiras, A. J. Stone, M. D. Su, and D. J. Tozer. *CADPAC: The Cambridge Analytical Derivatives Package.* Cambridge, UK, sixth edition, 1995.

[64] M. W. Schmidt, K. K. Baldridge, J. A. Boatz, J. H. Jensen, S. Koseki, M. S. Gordon, K. A. Nguyen, T. L. Windus, and S. T. Elbert. *QCPE Bull.*, 10:52, 1990.

[65] M. W. Schmidt, K. K. Baldridge, J. A. Boatz, S. T. Elbert, M. S. Gordon, J. H. Jensen, S. Koseki, N. Matsunaga, K. A. Nguyen, S. Su, T. L. Windus, and M. J. Dupuis. *J. Comput. Chem.*, 14:1347, 1993.

[66] P. J. Hay and W. R. Wadt. Ab initio effective core potentials for molecular calculations. Potentials for the transition metal atoms Sc to Hg. *J. Chem. Phys.*, 82:270–283, 1985.

[67] P. J. Hay and W. R. Wadt. Ab initio effective core potentials for molecular calculations. Potentials for main group elements Na to Bi. *J. Chem. Phys.*, 82:284–298, 1985.

[68] P. J. Hay and W. R. Wadt. Ab initio effective core potentials for molecular calculations. Potentials for K to Au including the outermost core orbitals. *J. Chem. Phys.*, 82:299–310, 1985.

[69] W. J. Stevens, H. Basch, and M. Krauss. Compact effective potentials and efficient shared-exponent basis sets for the first- and second-row atoms. *J. Chem. Phys.*, 81:6026–6033, 1984.

[70] W. J. Stevens, M. Krauss, H. Basch, and P. G. Jasien. Relativistic compact effective potentials and efficient shared-exponent basis sets for the third-, fourth- and fifth-row atoms. *Can. J. Chem.*, 70:612–630, 1992.

[71] T. R. Cundari and W. J. Stevens. Effective core potential methods for the lanthanides. *J. Chem. Phys.*, 98:5555–5565, 1993.

[72] M. J. Frisch, G. W. Trucks, H. B. Schlegel, P. M. W. Gill, B. G. Johnson, M. A. Robb, J. R. Cheeseman, T. Keith, G. A. Petersson, J. A. Montgomery, K. Raghavachari, M. A. Al-Laham, V. G. Zakrzewski, J. V. Ortiz, J. B. Foresman, J. Cioslowski, B. B. Stefanov, A. Nanayakkara M. Challacombe, C. Y. Peng, P. Y. Ayala, W. Chen, M. W. Wong, J. L. Andres, E. S. Replogle, R. Gomperts R. L. Martin, D. J. Fox, J. S. Binkey, D. J. DeFrees, J. Baker, J. J. P. Stewart, M. Head Gordon, C. Gonzalez, and J. A. Pople. *Gaussian 94*. Gaussian, Inc., Pittsburgh, PA, third edition, 1995.

[73] L. F. Pacios and P. A. Christiansen. Ab initio relativistic effective potentials with spin-orbit operators. 1. Li through Ar. *J. Chem. Phys.*, 82:2664–2671, 1985.

[74] M. M. Hurley, L. F. Pacios, P. A. Christiansen, R. B. Ross, and W. C. Ermler. Ab initio relativistic effective potentials with spin-orbit operators. 2. K through Kr. *J. Chem. Phys.*, 84:6840–6853, 1986.

[75] L. A. LaJohn, P. A. Christiansen, R. B. Ross, T. Atashroo, and W. C. Ermler. Ab initio relativistic effective potentials with spin-orbit operators. 3. Rb through Xe. *J. Chem. Phys.*, 87:2812–2824, 1987.

[76] R. B. Ross, J. M. Powers, T. Atashroo, W. C. Ermler, L. A. LaJohn, and P. A. Christiansen. Ab initio relativistic effective potentials with spin-orbit operators. 4. Cs through Rn. *J. Chem. Phys.*, 93:6654–6670, 1990.

[77] R. B. Ross, S. Gayen, and W. C. Ermler. Ab initio relativistic effective potentials with spin-orbit operators. 5. Ce through Lu. *J. Chem. Phys.*, 100:8145–8151, 1994.

[78] W. C. Ermler, R. B. Ross, and P. A. Christiansen. Ab initio relativistic effective potentials with spin-orbit operators. 6. Fr through Pu. *Int. J. Quantum Chem.*, 40:829–846, 1991.

[79] C. S. Nash, B. E. Bursten, and W. C. Ermler. Ab initio relativistic effective potentials with spin-orbit operators. 7. Am through element 118. *J. Chem. Phys.*, 106:5133–5142, 1997.

[80] M. Dolg, U. Wedig, H. Stoll, and H. Preuss. Energy-adjusted ab initio pseudopotentials for the 1st-row transition elements. *J. Chem. Phys.*, 86:866–872, 1987.

[81] G. Igelmann, H. Stoll, and H. Preuss. Pseudopotentials for main-group elements IIIA through VIIA. *Mol. Phys.*, 65:1321–1328, 1988.

[82] M. Dolg, H. Stoll, A. Savin, and H. Preuss. Energy-adjusted pseudopotentials for the rare-earth elements. *Theor. Chim. Acta*, 75:173–194, 1989.

[83] M. Dolg, H. Stoll, and H. Preuss. Energy-adjusted ab initio pseudopotentials for the rare-earth elements. *J. Chem. Phys.*, 90:1730–1734, 1989.

[84] D. Andrae, U. Haussermann, M. Dolg, H. Stoll, and H. Preuss. Energy-adjusted ab initio pseudopotentials for the 2nd and 3rd row transistion-elements. *Theor. Chim. Acta*, 77:123–141, 1990.

[85] D. Andrae, U. Haussermann, M. Dolg, H. Stoll, and H. Preuss. Energy-adjusted ab initio pseudopotentials for the 2nd and 3rd row transistion-elements – molecular test for Ag_2, Au_2 and RuH, OsH. *Theor. Chim. Acta*, 78:247–266, 1991.

[86] M. Dolg, W. Kuchle, H. Stoll, H. Preuss, and P. Schwerdtfeger. Ab initio pseudopotentials for Hg to Rn. 1. Parameter sets and atomic calculations. *Mol. Phys.*, 74:1245–1263, 1991.

[87] M. Dolg, W. Kuchle, H. Stoll, H. Preuss, and P. Schwerdtfeger. Ab initio pseudopotentials for Hg to Rn. 2. Molecular calculations on the hydrides of Hg to astatine and the fluorides of Rn. *Mol. Phys.*, 74:1265–1285, 1991.

[88] A. Bergner, M. Dolg, W. Kuchle, H. Stoll, and H. Preuss. Ab initio energy-adjusted pseudopotentials for elements of groups 13-17. *Mol. Phys.*, 80:1431–1441, 1993.

[89] W. Kuchle, M. Dolg, H. Stoll, and H. Preuss. Energy-adjusted pseudopotentials for the actinides – parameter sets and test calculations for thorium and thorium monoxide. *J. Chem. Phys.*, 100:7535–7542, 1993.

[90] R. Ahlrichs, M. Bar, M. Haser, H. Horn, and C. Kolmel. Electronic structure calculations on workstation computers – the program system TURBOMOLE. *Chem. Phys. Lett.*, 162:165–169, 1993.

[91] H. J. Werner and P. J. Knowles. *MOLPRO.* University of Birmingham, Birmingham, UK, 1998.

[92] N. R. Wallace, J. P. Blaudeau, and R. M. Pitzer. Optimized Gaussian basis sets for use with relativistic effective (core) potentials: Li-Ar. *Int. J. Quantum Chem.*, 40:789–796, 1991.

[93] J. P. Blaudeau and L. A. Curtis. Optimized gaussian basis sets for use with relativistic effective (core) potentials: K, Ca, Ga–Kr. *Int. J. Quantum Chem.*, 61:943-952, 1996.

[94] I. I. Tupitsyn, N. S. Mosyagin, and A. V. Titov. Generalized relativistic effective core potential. I. Numerical calculations for atoms Hg through Bi. *J. Chem. Phys.*, 103:6548-6555, 1995.

[95] J. M. L. Martin and A. Sundermann. Correlation consistent valence basis sets for use with the Stuttgart-Dresden-Bonn relativistic effective core potentials: The atoms Ga–Kr and In–Xe. *J. Chem. Phys.*, 114:3408–3420, 2001.

[96] C. Froese-Fischer. A multi-configuration Hartree-Fock program. *Comp. Phys. Comm.*, 1:151–166, 1969.

[97] C. Froese-Fischer. A multi-configuration Hartree-Fock program with improved stability. *Comp. Phys. Comm.*, 4:107–116, 1972.

[98] C. Froese-Fischer. *The Hartree-Fock Method for Atoms: A Numerical Approach.* John-Wiley & Sons, New York, 1977.

[99] S. Huzinaga and B. Miguel. A comparison of the geometrical sequence formula and the well-tempered formulas for generating GTO basis orbital exponents. *Chem. Phys. Lett.*, 175:289–291, 1990.

[100] P. A. M. Dirac. *Proc. Roy. Soc. A (London)*, 117:610, 1928.

[101] P. A. M. Dirac. *Proc. Roy. Soc. A (London)*, 118:315, 1928.

[102] S. Faas. *The ZORA approach in ab initio quantum chemistry.* PhD thesis, Universiteit Utrecht, The Netherlands, 2000.

[103] S. Faas, J. G. Snijders, J. H. van Lenthe, E. van Lenthe, and E. J. Baerends. The ZORA formalism applied to the Dirac-Fock equation. *Chem. Phys. Lett.*, 246:632-640, 1995.

[104] M. Douglas and N. M. Kroll. *Ann. Phys. (N.Y.)*, 82:89, 1974.

[105] B. A. Hess. Applicability of the no-pair equation with free-particle projection operators to atomic and molecular structure calculations. *Phys. Rev. A*, 32:756–763, 1985.

[106] B. A. Hess. Relativistic electronic-structure calculations employing a two-component no-pair formalism with external-field projection operators. *Phys. Rev. A*, 33:3742–3748, 1986.

[107] B. A. Hess. Revision of the Douglas-Kroll transformation. *Phys. Rev. A*, 39:6016–6017, 1989.

[108] K. G. Dyall. An exact separation of the spin-free and spin-dependent terms of the Dirac-Coulomb-Breit Hamiltonian. *J. Chem. Phys.*, 100:2118–2127, 1994.

[109] T. Nakajima and K. Hirao. A new relativistic theory: a relativistic scheme by eliminating small components(RESC). *Chem. Phys. Lett.*, 302:383–391, 1999.

[110] D. Fedorov, T. Nakajima, and K. Hirao. Analytic gradient for the relativistic elimination of small components(RESCs) approach. *Chem. Phys. Lett.*, 335:183–187, 2001.

[111] M. J. D. Powell. An efficient method for finding the minimum of a function of several variables without calculating derivatives. *Computer Journal*, 7:155–162, 1964.

[112] R. P. Brent. *Algorithms for minimization without derivatives.* Prentice-Hall, Englewood Cliffs, New Jersey, 1973.

[113] J. Y. Mane and M. Klobukowski. *Well-tempered Model Core Potentials: Part I. Non-relativistic parameters for main-group elements (Z=3–86).* Department of Chemistry, University of Alberta, Edmonton, 2001.

[114] J. Y. Mane and M. Klobukowski. *Well-tempered Model Core Potentials: Part II. Scalar-relativistic parameters (RESC) for main-group elements (Z=19–86).* Department of Chemistry, University of Alberta, Edmonton, 2001.

[115] G.L. Heard, C. J. Marsden, and G. E. Scuseria. *J. Phys. Chem.*, 96:4359, 1992.

[116] M. Kaupp, Ch. van Wüllen, R. Franke, F. Schmitz, and W. Kutzelnigg. *J. Am. Chem. Soc.*, 118:11939, 1996.

[117] T. D. Crawford, K. W. Springer, and H. F. Schaefer III. *J. Chem. Phys.*, 102:3307, 1995.

[118] A. J. Sadlej. Medium-sized polarized basis sets for high-level correlated calculations of molecular electric properties. I. *Collection Czech. Chem. Commun.*, 53:1995–2016, 1988.

[119] A. J. Sadlej. Medium-sized polarized basis sets for high-level correlated calculations of molecular electric properties. II. Second row atoms: Si through Cl. *Theor. Chim. Acta.*, 79:123–140, 1991.

[120] K. P. Huber and G. Herzberg. *Molecular Spectra and Molecular Structure*, volume 4. van Nostrand Reinhold, New York, 1979.

Appendix A

Supplementary Tables for Chapter 3

Table A.1: Comparison of wtMCP and experimental bond lengths and vibrational frequencies for group 13 halides (NR and SR represent NR-wtMCP and SR-wtMCP, respectively).

Molecule	Method	r_e/Å		$\overline{\omega}_e$/cm^{-1}	
		NR	SR	NR	SR
BF	RHF	1.2460		1491.69	
	MP2	1.2666		1400.97	
	DFT	1.2661		1346.83	
	EXP	1.2626		1402.13	
AlCl	RHF	2.1639		467.49	
	MP2	2.1646		469.64	
	DFT	2.1538		449.15	
	EXP	2.1301		481.30	
GaBr	RHF	2.3945	2.3936	255.77	253.42
	MP2	2.3490	2.3459	272.14	270.73
	DFT	2.3590	2.3586	260.92	259.15
	EXP	2.3525		263.00	
InI	RHF	2.8458	2.8305	163.30	161.70
	MP2	2.7757	2.7556	176.20	176.32
	DFT	2.7895	2.7740	171.48	170.72
	EXP	2.7537		177.1	

Table A.2: Comparison of wtMCP and experimental bond lengths and vibrational frequencies for group 14 sulfides (NR and SR represent NR-wtMCP and SR-wtMCP, respectively).

Molecule	**Method**	r_e/Å		$\overline{\omega}_e/\mathrm{cm}^{-1}$	
		NR	SR	NR	SR
CS	RHF	1.5251		1406.91	
	MP2	1.5586		1264.10	
	DFT	1.5432		1294.93	
	EXP	1.5349		1285.08	
SiS	RHF	1.9360		797.9	
	MP2	1.9780		717.86	
	DFT	1.9490		744.08	
	EXP	1.9293		749.64	
GeS	RHF	2.0020	1.9972	627.46	625.81
	MP2	2.0325	2.0276	570.51	569.23
	DFT	2.0101	2.0057	584.99	583.60
	EXP	2.0121		575.8	
SnS	RHF	2.2032	2.1951	538.95	535.02
	MP2	2.2357	2.2278	491.29	487.95
	DFT	2.2104	2.2039	500.23	496.44
	EXP	2.209		487.26	

Table A.3: Comparison of wtMCP and experimental bond lengths and vibrational frequencies for diatomic interhalogen compounds (NR and SR represent NR-wtMCP and SR-wtMCP, respectively).

Molecule	Method	r_e/Å		$\overline{\omega}_e/\text{cm}^{-1}$	
		NR	SR	NR	SR
ClF	RHF	1.6145		905.27	
	MP2	1.6741		769.16	
	DFT	1.6570		797.89	
	EXP	1.6283		786.15	
BrF	RHF	1.7286	1.7285	764.27	762.00
	MP2	1.7827	1.7824	662.85	662.00
	DFT	1.7681	1.7680	678.67	678.15
	EXP	1.7589		670.75	
BrCl	RHF	2.1460	2.1442	482.51	481.73
	MP2	2.1667	2.1648	449.19	448.74
	DFT	2.1513	2.1503	449.07	448.43
	EXP	2.1361		444.28	
IF	RHF	1.8820	1.8857	694.88	687.56
	MP2	1.9271	1.9305	617.71	612.62
	DFT	1.9190	1.9223	617.33	612.70
	EXP	1.9098		610.24	
ICl	RHF	2.3304	2.3284	416.10	414.32
	MP2	2.3453	2.3434	391.95	390.59
	DFT	2.3351	2.3337	386.01	384.86
	EXP	2.3209		384.29	
IBr	RHF	2.4846	2.4767	288.63	287.95
	MP2	2.4909	2.4831	272.10	271.93
	DFT	2.4848	2.4786	267.01	268.06
	EXP	2.469		268.64	

Table A.4: Comparison of wtMCP and experimental bond lengths and bond angles for dihydrogen chalcogenides (NR and SR represent NR-wtMCP and SR-wtMCP, respectively).

Molecule	Method	r_e/Å		ϕ(H-A-H)/degrees	
		NR	SR	NR	SR
OH_2	RHF	0.9440		105.88	
	MP2	0.9675		103.83	
	DFT	0.9634		103.94	
	EXP	0.9578		104.48	
SH_2	RHF	1.3421		93.93	
	MP2	1.3560		92.07	
	DFT	1.3528		92.02	
	EXP	1.3356		92.11	
SeH_2	RHF	1.4545	1.4516	93.06	92.77
	MP2	1.4584	1.4558	90.97	90.63
	DFT	1.4614	1.4596	90.86	90.56
	EXP	1.460		90.57	
TeH_2	RHF	1.6523	1.6451	92.72	92.18
	MP2	1.6480	1.6419	90.84	90.21
	DFT	1.6577	1.6524	90.62	90.14
	EXP	1.658		90.25	

Table A.5: Comparison of wtMCP and experimental bond lengths and bond angles for trihydrogen pnictides (NR and SR represent NR-wtMCP and SR-wtMCP, respectively).

Molecule	**Method**	r_e/Å		ϕ(H-A-H)/degrees	
		NR	SR	NR	SR
NH_3	RHF	1.0014		107.27	
	MP2	1.0187		106.02	
	DFT	1.0164		105.35	
	EXP	1.0016		106.68	
PH_3	RHF	1.4183		95.25	
	MP2	1.4294		93.37	
	DFT	1.4278		92.82	
	EXP	1.413		93.46	
AsH_3	RHF	1.5080	1.5051	94.44	94.09
	MP2	1.5085	1.5057	92.33	91.94
	DFT	1.5141	1.5122	91.74	91.40
	EXP	1.513		92.09	
SbH_3	RHF	1.7059	1.6971	94.26	93.56
	MP2	1.7004	1.6921	92.51	91.70
	DFT	1.7096	1.7032	91.85	91.59
	EXP	1.7039		91.6	

Appendix B

Supplementary Figures for Chapter 2

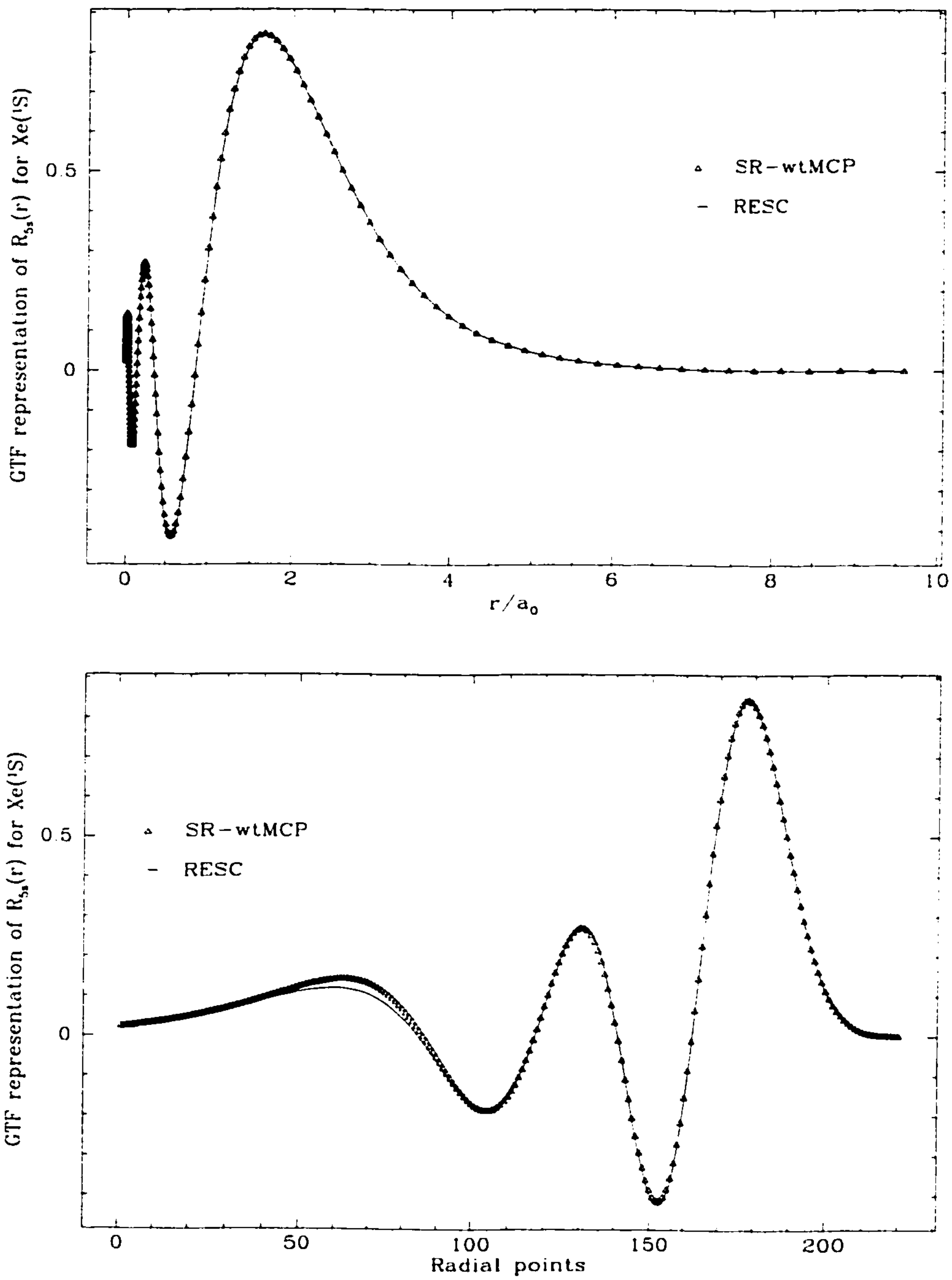

Figure B.1: Scalar-relativistic Xe(^{1}S) $5s$ radial distribution function

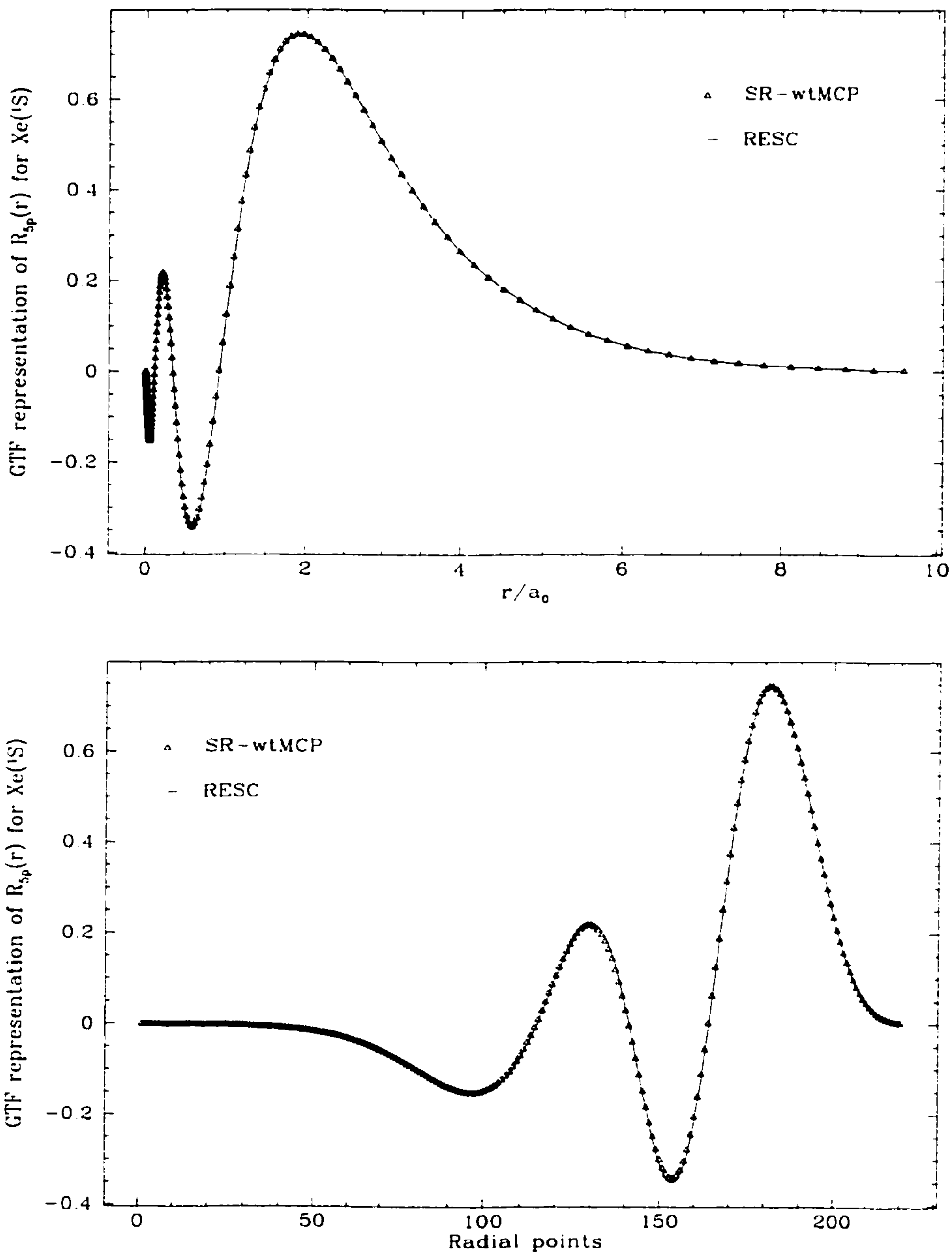

Figure B.2: Scalar-relativistic $Xe(^1S)$ $5p$ radial distribution function

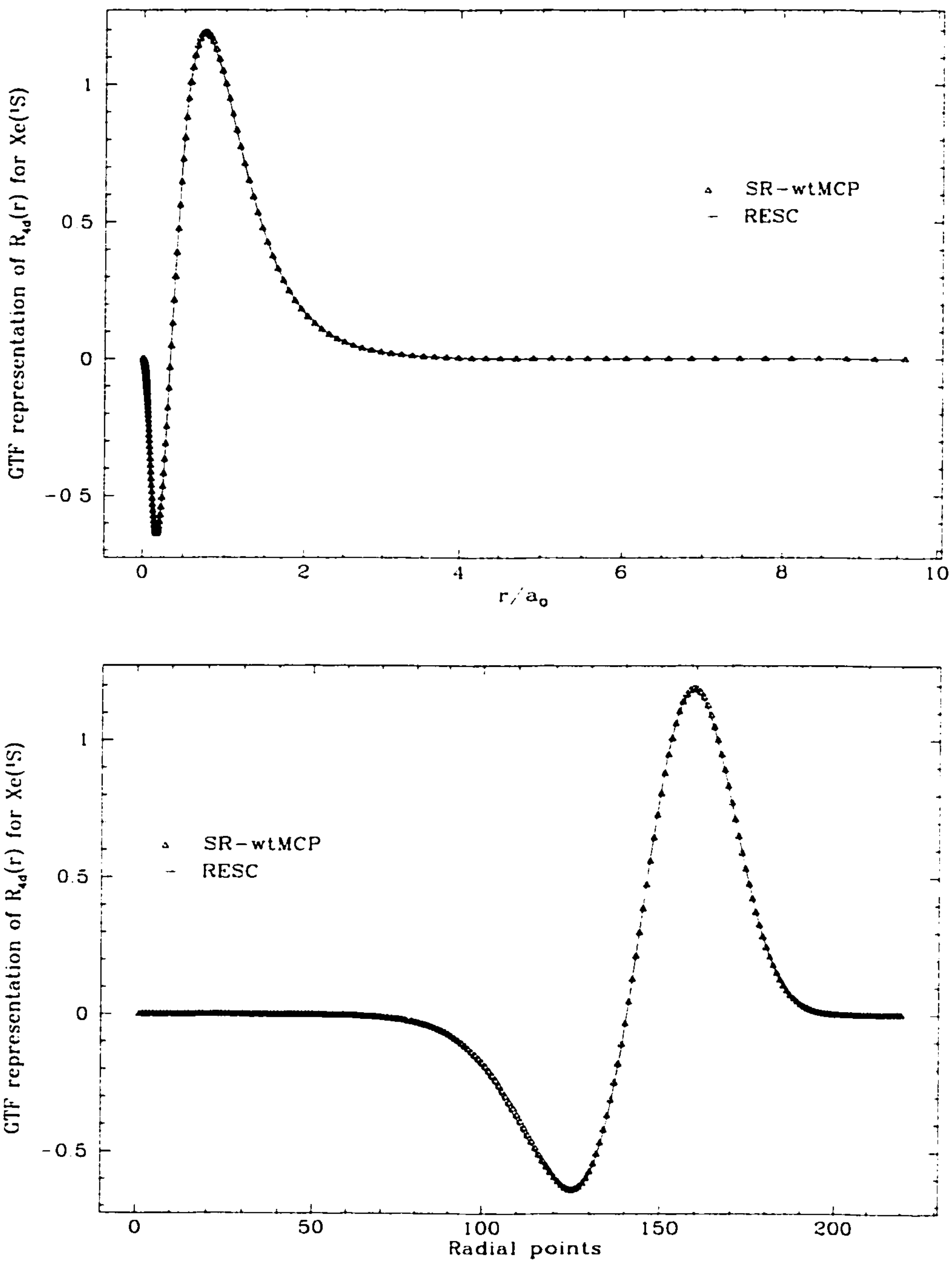

Figure B.3: Scalar-relativistic Xe(^{1}S) $4d$ radial distribution function